

**EFFECTS OF AGGREGATE TYPE, SIZE, AND  
CONTENT ON CONCRETE STRENGTH AND FRACTURE ENERGY**

**By  
Rozalija Kozul  
David Darwin**

**A Report on Research Sponsored by**

**THE NATIONAL SCIENCE FOUNDATION  
Research Grants No. MSS-9021066 and CMS-9402563**

**THE U.S. DEPARTMENT OF TRANSPORTATION  
FEDERAL HIGHWAY ADMINISTRATION**

**THE REINFORCED CONCRETE RESEARCH COUNCIL  
Project 56**

**Structural Engineering and Engineering Materials  
SM Report No. 43**

**UNIVERSITY OF KANSAS CENTER FOR RESEARCH, INC.  
LAWRENCE, KANSAS**

**June 1997**



## ABSTRACT

The effects of aggregate type, size, and content on the behavior of normal and high-strength concrete, and the relationships between compressive strength, flexural strength, and fracture energy are discussed. The concrete mixtures incorporate either basalt or crushed limestone, aggregate sizes of 12 mm ( $\frac{1}{2}$  in.) or 19 mm ( $\frac{3}{4}$  in.), and coarse aggregate contents with aggregate volume factors (ACI 211.1-91) of 0.75 and 0.67. Water-to-cementitious material ratios range from 0.24 to 0.50. Compressive strengths range from 25 MPa (3,670 psi) to 97 MPa (13,970 psi).

Compression test results show that high-strength concrete containing basalt produces slightly higher compressive strengths than high-strength concrete containing limestone, while normal-strength concrete containing basalt yields slightly lower compressive strengths than normal-strength concrete containing limestone. The compressive strength of both normal and high-strength concrete is little affected by aggregate size. High-strength concrete containing basalt and normal-strength concrete containing basalt or limestone yield higher compressive strengths with higher coarse aggregate contents than with lower coarse aggregate contents. The compressive strength of high-strength concrete containing limestone is not affected by aggregate content.

Flexure test results show that high-strength concrete containing basalt yields higher flexural strengths than concrete with similar compressive strength containing limestone. The flexural strength of high-strength concrete containing limestone is limited by the strength of the rock and the matrix. The flexural strength of high-strength concrete containing basalt is controlled by the strength of the rock and the interfacial strength at the matrix-aggregate interface. The flexural strength of normal-strength concrete containing the basalt or limestone used in this study is not affected by aggregate type, and is limited by the matrix strength and the strength of the interfacial transition zone. The flexural strength of normal and high-strength concrete is not affected by aggregate size. Normal and high-strength concretes containing basalt yield higher flexural strengths with higher coarse aggregate contents than with

lower coarse aggregate contents.

Fracture energy test results show that normal and high-strength concretes containing basalt yield significantly higher fracture energies than concretes containing limestone. The fracture energy of high-strength concrete decreases with an increase in aggregate size, while the fracture energy of normal-strength concrete increases with an increase in aggregate size. High-strength concrete containing basalt and normal-strength concrete containing limestone yield higher fracture energies with higher coarse aggregate content than with lower coarse aggregate contents. The fracture energy of high-strength concrete containing limestone and normal-strength concrete containing basalt is not affected by aggregate content.

There is no well-defined relationship between fracture energy and compressive strength, or fracture energy and flexural strength. However, there is a close relationship between the peak bending stresses obtained in the flexure and fracture tests.

**Keywords:** aggregates; compression; concrete; cracking (fracturing); flexure; fracture energy; fracture mechanics; high-strength concrete; strength; tension; tests.

## ACKNOWLEDGEMENTS

This report is based on a thesis submitted by Rozalija Kozul in partial fulfillment of the requirements of the M.S.C.E. degree. Support for this research was provided by the National Science Foundation under NSF Grants No. MSS-9021066 and CMS-9402563, the U.S. Department of Transportation – Federal Highway Administration, the Reinforced Concrete Research Council under RCRC Project 56, and the Lester T. Sunderland Foundation. The basalt coarse aggregate was supplied by Geiger Ready-Mix and Iron Mountain Trap Rock Company. Additional support was provided by Richmond Screw Anchor Company.



## TABLE OF CONTENTS

	<u>Page</u>
ABSTRACT.....	i
ACKNOWLEDGEMENTS.....	iii
LIST OF TABLES.....	vi
LIST OF FIGURES.....	vii
CHAPTER 1 INTRODUCTION.....	1
1.1 General.....	1
1.2 Background.....	2
1.3 Previous Work.....	3
1.4 Summary.....	11
1.5 Object and Scope.....	12
CHAPTER 2 EXPERIMENTAL WORK.....	13
2.1 Materials.....	13
2.2 Preparation.....	14
2.3 Testing.....	15
CHAPTER 3 RESULTS.....	17
3.1 Compression Test Results.....	17
3.2 Flexure Test Results.....	21
3.3 Fracture Energy Test Results.....	24
3.4 Flexural Strength versus Compressive Strength.....	30
3.5 Fracture Energy versus Compressive Strength.....	31
3.6 Fracture Energy versus Flexural Strength.....	33
3.7 Bending Stress -- Fracture Test versus Flexural Strength.....	33
CHAPTER 4 EVALUATION.....	35
4.1 Compression Test Evaluation.....	35
4.2 Flexure Test Evaluation.....	38
4.3 Fracture Energy Test Evaluation.....	40

4.4	Flexural Strength - Compressive Strength Relationship.....	43
4.5	Fracture Energy - Compressive Strength Relationship.....	44
4.6	Fracture Energy - Flexural Strength Relationship.....	44
4.7	Bending Stress -- Fracture Test - Flexural Strength.....	45
CHAPTER 5 SUMMARY AND CONCLUSIONS.....		46
5.1	Summary.....	46
5.2	Conclusions.....	46
5.3	Future Work.....	48
REFERENCES.....		50
APPENDIX A Details of Fracture Test Specimens.....		82



**LIST OF TABLES**

	<u>Page</u>
2.1 Mix Proportions (S.I. Units).....	53
2.2 Mix Proportions (Customary Units).....	54
3.1 Compression Test Results.....	55
3.2 Flexure Test Results.....	56
3.3 Fracture Energy Test Results.....	57
3.4 Bending Stress Results.....	58
A.1 Details of Fracture Test Specimens (S.I. Units).....	82
A.2 Details of Fracture Test Specimens (Customary Units).....	84

## LIST OF FIGURES

	<u>Page</u>
2.1 Fracture energy test setup.....	59
3.1 Schematic representation of fracture energy test specimen.....	60
3.2 Fracture specimen load-deflection curves for basalt and limestone high-strength concretes -- high aggregate content (HB-12h.3 and HL-12h.2).....	61
3.3 Fracture specimen load-deflection curves for basalt and limestone normal-strength concretes -- high aggregate content (NB-12h and NL-12h).....	62
3.4 Fracture specimen load-deflection curves for basalt and limestone normal-strength concretes -- low aggregate content (NB-12l and NL-12l).....	63
3.5 Profile of fracture surfaces for basalt and limestone normal and high-strength concretes -- 12 mm (1/2 in.) high aggregate content.....	64
3.6 Fracture specimen load-deflection curves for 12 mm (1/2 in.) and 19 mm (3/4 in.) basalt high-strength concretes -- high aggregate content (HB-12h.2 and HB-19h.1).....	65
3.7 Fracture specimen load-deflection curves for 12 mm (1/2 in.) and 19 mm (3/4 in.) basalt high-strength concretes -- high aggregate content (HB-12h.3 and HB-19h.2).....	66
3.8 Fracture specimen load-deflection curves for 12 mm (1/2 in.) and 19 mm (3/4 in.) basalt normal-strength concretes -- high aggregate content (NB-12h and NB-19h).....	67
3.9 Fracture specimen load-deflection curves for high and low basalt aggregate contents -- high-strength concrete (HB-12h.1 and HB-12l.1).....	68

3.10	Fracture specimen load-deflection curves for high and low basalt aggregate contents -- high-strength concrete (HB-12h.3 and HB-12l.2).....	69
3.11	Fracture specimen load-deflection curves for high and low limestone aggregate contents -- high-strength concrete (HL-12h.2 and HL-12l).....	70
3.12	Fracture specimen load-deflection curves for high and low basalt aggregate contents -- normal-strength concrete (HB-12h.3 and HB-12l.2).....	71
3.13	Fracture specimen load-deflection curves for high and low limestone aggregate contents -- normal-strength concrete (HL-12h.2 and HL-12l).....	72
3.14	Flexural strength versus compressive strength for normal and high-strength concretes.....	73
3.15	Fracture energy versus compressive strength for normal and high-strength concretes.....	74
3.16	Fracture specimen load-deflection curves for normal and high-strength concretes containing 19 mm (3/4 in.) basalt -- high aggregate content (HB-19h.1 and NB-19h).....	75
3.17	Fracture specimen load-deflection curves for normal and high-strength concretes containing 12 mm (1/2 in.) basalt -- high aggregate content (HB-12h.3 and NB-12h).....	76
3.18	Fracture specimen load-deflection curves for normal and high-strength concretes containing 12 mm (1/2 in.) basalt -- low aggregate content (HB-12l.2 and NB-12l).....	77
3.19	Fracture specimen load-deflection curves for normal and high-strength concretes containing 12 mm (1/2 in.) limestone -- high aggregate content (HL-12h.2 and NL-12l).....	78

3.20	Fracture specimen load-deflection curves for normal and high-strength concretes containing 12 mm (1/2 in.) limestone -- low aggregate content (HL-12l and NL-12l).....	79
3.21	Fracture energy versus flexural strength for normal and high-strength concretes.....	80
3.22	Bending stress relationship for fracture and flexural strength tests.....	81

# CHAPTER 1

## INTRODUCTION

### 1.1 GENERAL

It is well recognized that coarse aggregate plays an important role in concrete. Coarse aggregate typically occupies over one-third of the volume of concrete, and research indicates that changes in coarse aggregate can change the strength and fracture properties of concrete. To predict the behavior of concrete under general loading requires an understanding of the effects of aggregate type, aggregate size, and aggregate content. This understanding can only be gained through extensive testing and observation.

There is strong evidence that aggregate type is a factor in the strength of concrete. Ezeldin and Aitcin (1991) compared concretes with the same mix proportions containing four different coarse aggregate types. They concluded that, in high-strength concretes, higher strength coarse aggregates typically yield higher compressive strengths, while in normal-strength concretes, coarse aggregate strength has little effect on compressive strength. Other research has compared the effects of limestone and basalt on the compressive strength of high-strength concrete (Giaccio, Rocco, Violini, Zappitelli, and Zerbino 1992). In concretes containing basalt, load-induced cracks developed primarily at the matrix-aggregate interface, while in concretes containing limestone, nearly all of the coarse aggregate particles were fractured. Darwin, Tholen, Idun, and Zuo (1995, 1996) observed that concretes containing basalt coarse aggregate exhibited higher bond strengths with reinforcing steel than concretes containing limestone.

There is much controversy concerning the effects of coarse aggregate size on concrete, principally about the effects on fracture energy. Some research (Strange and Bryant 1979, Nallathambi, Karihaloo, and Heaton 1984) has shown that there is an increase in fracture toughness with an increase in aggregate size. However, Gettu and Shah (1994) have stated that, in some high-strength concretes where the coarse aggregates rupture during fracture, size is not expected to influence the fracture

parameters. Tests by Zhou, Barr, and Lydon (1995) show that compressive strength increases with an increase in coarse aggregate size. However, most other studies disagree. Walker and Bloem (1960) and Bloem and Gaynor (1963) concluded that an increase in aggregate size results in a decrease in the compressive strength of concrete. Cook (1989) showed that, for compressive strengths in excess of 69 MPa (10,000 psi), smaller sized coarse aggregate produces higher strengths for a given water-to-cement ratio. In fact, it is generally agreed that, although larger coarse aggregates can be used to make high-strength concrete, it is easier to do so with coarse aggregates below 12.5 mm (½ in.) (ACI 363-95).

There has not been much research on the effects of coarse aggregate content on the fracture energy of concrete. One study, conducted by Moavenzadeh and Kuguel (1969), found that fracture energy increases with the increase in coarse aggregate content. Since cracks must travel around the coarse aggregate particles, the area of the crack surface increases, thus increasing the energy demand for crack propagation. There is controversy, however, on the effects of coarse aggregate content on the compressive strength of concrete. Ruiz (1966) found that the compressive strength of concrete increases with an increase in coarse aggregate content until a critical volume is reached, while Bayasi and Zhou (1993) found little correlation between compressive strength and coarse aggregate content.

In light of the controversy, this report describes work that is aimed at improving the understanding of the role that coarse aggregate plays in the compressive, tensile, and fracture behaviors of concrete.

## 1.2 BACKGROUND

The role of coarse aggregate in concrete is central to this report. While the topic has been under study for many years, an understanding of the effects of coarse aggregate has become increasingly more important with the introduction of high-strength concretes, since coarse aggregate plays a progressively more important role

in concrete behavior as strength increases.

In normal-strength concrete, failure in compression almost exclusively involves debonding of the cement paste from the aggregate particles at what, for the purpose of this report, will be called the matrix-aggregate interface. In contrast, in high-strength concrete, the aggregate particles as well as the interface undergo failure, clearly contributing to overall strength. As the strength of the cement paste constituent of concrete increases, there is greater compatibility of stiffness and strength between the normally stiffer and stronger coarse aggregate and the surrounding mortar. Thus, microcracks tend to propagate through the aggregate particles since, not only is the matrix-aggregate bond stronger than in concretes of lower strength, but the stresses due to a mismatch in elastic properties are decreased. Thus, aggregate strength becomes an important factor in high-strength concrete.

This report describes work that is aimed at improving the understanding of the role of aggregates in concrete. The variables considered are aggregate type, aggregate size, and aggregate content in normal and high-strength concretes. Compression, flexural, and fracture tests are used to better understand the effects aggregates have in concrete.

### 1.3 PREVIOUS WORK

Kaplan (1959) studied the effects of the properties of 13 coarse aggregates on the flexural and compressive strength of high-strength and normal-strength concrete. At all ages, flexural strengths for basalt mixes were higher than limestone mixes with the same mix proportions. The compressive strength for basalt mixes was also higher than limestone mixes; however, the difference in strength was less notable in concretes of higher strength. The flexural strength-to-compressive strength ratios for both basalt and limestone mixes ranged from 9 to 12 percent. Kaplan also observed that concrete with 91-day strengths in excess of 69 MPa (10,000 psi) yielded lower flexural strengths than mortar of the same mix proportions; however, concretes below 69 MPa

(10,000 psi) yielded similar flexural strengths to mortar of the same mix proportions. Kaplan also observed, contrary to most results, that concrete with compressive strengths greater than 69 MPa (10,000 psi) was generally greater than mortar of the same mix proportions, indicating that at very high strengths, the presence of coarse aggregate contributed to the ultimate compressive strength of concrete.

Walker and Bloem (1960) studied the effects of coarse aggregate size on the properties of normal-strength concrete. Their work demonstrates that an increase in aggregate size from 10 to 64 mm ( $\frac{3}{8}$  to  $2\frac{1}{2}$  in.) results in a decrease in the compressive strength of concrete, by as much as 10 percent; however, aggregate size seems to have negligible effects on flexural strength. The study also shows that the flexural-to-compressive strength ratio remains at approximately 12 percent for concrete with compressive strengths between 35 MPa (5,100 psi) and 46 MPa (6,700 psi).

Bloem and Gaynor (1963) studied the effects of size and other coarse aggregate properties on the water requirements and strength of concrete. Their results confirm that increasing the maximum aggregate size reduces the total surface area of the aggregate, thus reducing the mixing water requirements; however, even with the reduction in water, a larger size aggregate still produces lower compressive strengths in concrete compared to concretes containing smaller aggregate. Generally, in lower strength concretes, the reduction in mixing water is sufficient to offset the detrimental effects of aggregate size. However, in high-strength concretes, the effect of size dominates, and the smaller sizes produce higher strengths.

Cordon and Gillespie (1963) also reported changes in concrete strength for mixes made with various water-to-cement ratios and aggregate sizes. They found that, at water-to-cement ratios from 0.40 to 0.70, an increase in maximum aggregate size from 19 mm ( $\frac{3}{4}$  in.) to 38 mm ( $1\frac{1}{2}$  in.) decreases the compressive strength by about 30 percent. They also concluded that, in normal-strength concrete, failure typically occurs at the matrix-aggregate interface and that the stresses at the interface which cause failure can be reduced by increasing the surface area of the aggregate (decreasing the aggregate size). If the strength of the concrete is sufficiently high, such as with high-strength concrete, failure of the specimen is usually accompanied by the fracture of



aggregate particles; therefore, in high-strength concrete, compressive strength depends on aggregate strength, not necessarily aggregate size.

In research on the effects of aggregate content on the behavior of concrete, Ruiz (1966) found that the compressive strength of concrete increases along with an increase in coarse aggregate content, up to a critical volume of aggregate, and then decreases. The initial increase is due to a reduction in the volume of voids with the addition of aggregate.

Moavenzadeh and Kuguel (1969) tested notched-beam three-point bend specimens of cement paste, mortar, and concrete to review the applicability of brittle fracture concepts to concrete and to determine fracture mechanics parameters for the three materials. The results of the study show that the work of fracture increases as aggregate content increases. Since cracks that form in cement paste specimens propagate in a straight path, fracture energy in these specimens is low. However, for mortar and concrete, the crack follows a meandering path, tending to go around rather than through the aggregates. The meandering path increases the energy required for crack propagation, since the area of the cracked surface is increased.

Using three-point bend tests, Strange and Bryant (1979) investigated the interaction of matrix cracks and aggregate particles in concrete with compressive strengths greater than 70 MPa (10,150 psi). They found an increase in fracture toughness with an increase in aggregate size. As a crack meets an aggregate particle, it passes along the matrix-aggregate interface, and then re-enters the matrix. Larger aggregate particles result in a greater increase in crack surface than smaller particles and, thus, require more energy for crack propagation. However, although they found an increase in fracture toughness with an increase in aggregate size, the study shows a decrease in flexural strength with an increase in aggregate size.

Compression-induced microcracking was studied by Carrasquillo, Slate, and Nilson (1981) for concretes with compressive strengths ranging from 31 to 76 MPa (4500 to 11,000 psi). They found that, in lower strength concretes, the weakest link almost exclusively occurs at the matrix-aggregate interface and the mechanism of progressive microcracking consists of mortar cracks bridging between nearby bond

cracks. High-strength concretes had fewer and shorter microcracks at all strains than did normal-strength concretes. The observed behavior is explained by viewing high-strength concrete as a more homogeneous material. When the matrix is more compact and the voids are less in number, there is greater compatibility between the strength and elastic properties of the coarse aggregate and the mortar. Improved compatibility also lowers the stress at the matrix-aggregate interface, reducing the likelihood of interfacial failure. Thus, microcracks are more likely to propagate through the aggregate, and therefore, the extent of microcracking is reduced as concrete strength increases.

The mechanical properties of concretes with compressive strengths ranging from 21 to 62 MPa (3,000 to 9,000 psi) were also studied by Carrasquillo, Nilson, and Slate (1981). Flexural strength tests, using third point loading, were performed on normal, medium, and high-strength limestone aggregate concrete. The results show that the amount of aggregate fracture along the plane of failure is substantially larger for high-strength concrete than for normal-strength concrete. The authors also conclude that, in high-strength concrete, the greater stiffness of the mortar constituent and the higher matrix-aggregate tensile bond strength cause the observed increase in the modulus of elasticity.

Tests were conducted by Nallathambi, Karihaloo, and Heaton (1984) on mortar and concrete beams of normal strength to examine the influence of specimen dimension, notch depth, aggregate size (10 mm, 14 mm and 20 mm), and water-to-cement ratio on the fracture behavior of concrete. They demonstrated that, along with compressive strength and elastic modulus, fracture toughness increases about 38 percent with a decrease in water-to-cement ratio of 23 percent. They also showed that fracture toughness increases with an increase in the maximum size of coarse aggregate. They stated that microcracking and matrix-aggregate debonding during the process of crack propagation consumes considerable energy; therefore, the larger the aggregate, the larger the crack area, increasing the energy demand required for crack growth.

Bentur and Mindess (1986) compared crack patterns in different types of plain concrete subjected to bending as a function of loading rate. They observed that,

regardless of the loading rate, cracks in normal-strength concrete tend to form around the aggregate particles, passing along the matrix-aggregate interface. In high-strength concrete, the crack path is similar to that of normal-strength concrete when loaded at a low rate (1 mm/min) during a three-point bending test. However, at a higher loading rate (250 mm/min), cracks propagate through the aggregate particles, resulting in straight crack paths. This behavior can be explained by suggesting that when energy is introduced into a system in a very short period, cracks are forced to develop along shorter paths of higher resistance, thus, resulting in cracks propagating through aggregate particles.

The effects of admixture dosage, mix proportions, and coarse aggregate size on concretes with strengths in excess of 69 MPa (10,000 psi) were discussed by Cook (1989). The two maximum size aggregates studied were a 10 mm ( $\frac{3}{8}$  in.) and a 25 mm (1 in.) limestone. The smaller sized coarse aggregate produced higher compressive strengths than the larger sized coarse aggregate. Cook observed that the difference in compressive strengths due to aggregate size is increasingly larger with a decreasing water-to-cement ratio and increasing test age. The smaller sized coarse aggregate also increases the flexural strength of the concrete. The flexural-to-compressive strength ratio remains constant at approximately 12 percent. The test specimens exhibited increases in the modulus of elasticity of approximately 20 percent between 7 to 90 days for the 10 mm ( $\frac{3}{8}$  in.) limestone, and 13 percent for the 25 mm (1 in.) limestone.

Gettu, Bazant, and Karr (1990) studied the fracture properties and brittleness of concrete with compressive strengths in excess of 84 MPa (12,200 psi) using three-point bend specimens. They have observed that cracks in high-strength concrete containing gravel propagated through the coarse aggregate, while cracks in normal-strength concrete propagated mainly along the matrix-aggregate interface. The reduced crack area is due to the strong matrix-aggregate bond and the strength of the matrix itself, which approaches the strength of the aggregates, resulting in a more homogeneous behavior. They observed, however, that a 160 percent increase in compressive strength results in an increase in fracture energy of only 12 percent.

In a study of the effects of coarse aggregate type and size on the compressive

strength of normal and high-strength concrete, Ezeldin and Aitcin (1991) concluded that normal-strength concretes are not greatly affected by the type or size of coarse aggregates. However, for high-strength concretes, coarse aggregate type and size affect the strength and failure mode of concrete in compression. For high-strength concretes with weaker coarse aggregates, cracks pass through the aggregates, since the matrix-aggregate bond is stronger than the aggregate itself, resulting in a transgranular type of failure. For high-strength concretes with stronger aggregates, both matrix-aggregate debonding and transgranular failure occur. They found that cracks pass through the weaker portions of aggregate particles and then propagate into the cement paste. They also observed that the coarse aggregate types and sizes used in the study did not significantly affect the flexural strength of high-strength concrete.

Giaccio, Rocco, Violini, Zappitelli, and Zerbino (1992) studied the effect of coarse aggregate type (basalt, granite and limestone) on the mechanical properties of high-strength concrete. Compressive and flexural strength, modulus of elasticity, and stress-strain behavior were analyzed for concrete, mortar, and rock. They found that weaker aggregates, such as limestone, reduce compressive strengths significantly, since the concrete strength is limited by the aggregate strength. However, aggregate type did not affect flexural strength. Comparing fractured surfaces for the concretes shows that nearly all of the exposed coarse aggregate particles are fractured in the limestone mixes. However, cracks form primarily at the matrix-aggregate interface, and only a few aggregate particles are fractured in the basalt mix. The highest modulus of elasticity was achieved in the basalt mix, followed by limestone and granite. The basalt mix also showed the highest compressive strength, followed by granite and limestone. The granite mix had the best elastic compatibility between the matrix and aggregate, but the granite had significantly lower tensile strength than the basalt.

Giaccio, Rocco, and Zerbino (1993) compared fracture energies for concretes with a wide range of compressive strengths. Strength levels from 22 MPa (3,190 psi) to 100 MPa (14,500 psi), aggregate type (basalt, limestone and gravel), aggregate size (8 mm, 16 mm and 32 mm), and aggregate surface roughness were included as

variables. They concluded that concretes with weaker aggregates, such as limestone, yield lower compressive strengths than concrete with stronger coarse aggregate. Fracture energy increases as concrete compressive strength increases, although the increase in energy of only 4 percent corresponds to an increase of in strength of 10 percent. They also concluded that fracture energy increases with increasing aggregate size. Load-deflection curves for fracture energy were also analyzed. They show that, as the compressive strength increases, concretes have a greater peak load followed by a steeper gradient of the softening branch. They also show that the final deflection (at total fracture) is much lower for high-strength mortar than for high-strength concrete. The mortar specimens had the steepest gradient of the descending branch, followed by concretes containing basalt and limestone coarse aggregates.

A study of various properties of concrete containing silica fume was reported by Bayasi and Zhou (1993). The effects of aggregate content, aggregate gradation, water-to-cementitious material ratio, and superplasticizer dosage rate were also discussed. They concluded that aggregate content seems to have a relatively negligible effect on the compressive strength of silica fume concrete. However, aggregates work to arrest cracks when concrete is subjected to flexural loads; therefore, increasing aggregate content increases the flexural strength of concrete.

Zhou, Barr, and Lydon (1995) studied the fracture properties of concretes with compressive strengths ranging from 80 to 115 MPa (11,600 to 16,700 psi). Mixtures with water-to-cementitious material ratios of 0.23 and 0.32 and 10% and 15% silica fume replacements of cement (by weight) were compared. Concretes made with 10 mm (0.4 in.) gravel and 10 mm (0.4 in.) and 20 mm (0.8 in.) crushed limestone were also compared. Zhou et al. concluded that, in contrast to other studies, *increasing* the coarse aggregate size from 10 mm (0.4 in.) to 20 mm (0.8 in.) increases the compressive strength of the concrete by about 10 percent. They also found that, similar to normal-strength concrete, the fracture energy of high-strength concrete increases with increasing aggregate size. However, also in contrast to other studies, they observed a *decrease* in fracture energy with increasing compressive strength. They concluded that the fracture energy decrease may be due to the improvement in

the matrix-aggregate bond which results in cracks developing through aggregates rather than passing along the matrix-aggregate interface.

Xie, Elwi, and MacGregor (1995) investigated the mechanical properties of 60, 90, and 120 MPa (8,700, 13,000, and 17,400 psi) concretes. The objective was to determine the compressive cylinder strength, split-cylinder tensile strength, fracture energy using notched beams, and the maximum and residual triaxial strengths. Load-deflection curves for fracture energy were analyzed. They show that an increase in compressive strength of concrete increases the peak load of the curve followed by a steeper gradient of the softening branch. They also found that an increase in compressive strength of about 25 percent corresponds with an increase in fracture energy of only 10 percent.

Perdikaris and Romeo (1995) investigated the effect of beam size, aggregate size, and compressive strength on the fracture energy of plain concrete. Concretes with cylinder compressive strengths of 28 MPa (4,000 psi) and 55 MPa (8,000 psi) and maximum aggregate sizes of 6 mm ( $\frac{1}{4}$  in.) and 25 mm (1 in.) were tested. The results indicate that aggregate size has a considerable influence on fracture energy. For both the normal and the high-strength concretes with 25 mm (1 in.) aggregate, fracture energy was about twice the fracture energy of the concretes containing 6 mm ( $\frac{1}{4}$  in.) aggregate. They concluded that, for concrete with the larger aggregate, there is a higher degree of matrix-aggregate interlock, resulting in an increase in the energy required for crack propagation.

Maher and Darwin (1976, 1977) observed that the bond strength between the interfacial region and aggregate plays a less dominant role in the compressive strength of concrete than generally believed. Finite element models were used to evaluate the effect of matrix-aggregate bond strength on the strength of concrete. They observed that an increase in bond strength from normal values to perfect bond (no failure at the interface) resulted in only a 4 percent increase in compressive strength of the model. A decrease to zero interfacial strength resulted in a decrease in compressive strength of just 11 percent. The lack of sensitivity in bond strength to changes in water-to-cement ratio, demonstrated in earlier tests (Hsu and Slate 1963, Taylor and Broms

1964), provides strong support for the matrix, rather than the interface, as the principal controlling factor in the strength of concrete.

#### 1.4 SUMMARY

The following summarizes the findings of previous research work on the effects of aggregate type, size, and content on normal and high-strength concretes:

##### Type

1. In high-strength concretes, higher strength coarse aggregates typically yield higher compressive strengths and fracture energy, while in normal-strength concretes, coarse aggregate strength has little effect on compressive strength or fracture energy.
2. Most researchers conclude that aggregate type has little affect on flexural strength; however, other researchers argue that higher strength coarse aggregates yield higher flexural strengths than lower strength coarse aggregates.

##### Size

1. In high-strength concretes, a smaller maximum aggregate size yields higher compressive strengths; however, in normal-strength concretes, aggregate size has much less effect on compressive strength.
2. Most researchers conclude that an increase in maximum aggregate size lowers the flexural strength of concrete; however, some researchers argue that aggregate size has negligible effects on flexural strength.
3. Researchers have shown an increase in fracture energy with an increase in aggregate size; however, others have stated that in some high-strength concretes where the coarse aggregates rupture during fracture, size is not expected to influence the fracture parameters.

### Content

1. Most researchers conclude that an increase in aggregate content decreases the compressive strength; however, research has demonstrated that an increase in aggregate content, until a critical volume is attained, increases the compressive strength.
2. No conclusive research has been found on the effects of aggregate content on flexural strength.
3. An increase in aggregate content increases the fracture energy of concrete.

### **1.5 OBJECT AND SCOPE**

The purpose of this research is to compare the compressive strength, flexural strength, and fracture energy of normal and high-strength concretes with different aggregate types, sizes, and contents.

Compressive strengths range from 25 MPa (3,670 psi) to 97 MPa (13,970 psi). Fifteen batches (5 normal-strength concrete and 10 high-strength concrete) of 9 specimens each were tested. Some data cannot be used due to errors during testing. The results of 45 compression, 45 flexural, and 42 fracture energy tests are reported.



## CHAPTER 2

### EXPERIMENTAL WORK

To study the effects of coarse aggregate type, size, and content on the behavior of concrete, prismatic specimens were tested in compression, in flexure using center-point loading, and a three-point bending test on notched beams. The concrete mixtures incorporated either basalt or crushed limestone, aggregate sizes of 12 mm ( $\frac{1}{2}$  in.) or 19 mm ( $\frac{3}{4}$  in.), and coarse aggregate contents with aggregate volume factors (ACI 211.1-91) of 0.75 and 0.67. Water-to-cementitious material ratios ranged from 0.24 to 0.50.

#### 2.1 MATERIALS

Type I portland cement, silica fume, and fly ash were used in the concrete mixtures. The dry, compacted silica fume (Master Builders MB-SF) contained 92 percent  $\text{SiO}_2$ , 0.45 percent  $\text{Na}_2\text{O}$ , 0.36 percent  $\text{SO}_3$ , 0.10 percent  $\text{Cl}$ , and 0.52 percent loss on ignition. The Class C fly ash, supplied by Flinthills Fly Ash, contained 34 percent  $\text{SiO}_2$ , 29 percent  $\text{CaO}$ , 20 percent  $\text{Al}_2\text{O}_3$ , 7 percent  $\text{MgO}$ , 4 percent  $\text{Fe}_2\text{O}_3$ , and 3 percent  $\text{SO}_3$ .

The fine aggregate was Kansas river sand with a fineness modulus = 2.60; bulk specific gravity (saturated surface dry) = 2.62; and absorption (dry) = 0.5 percent. The sand passed through a No. 4 sieve prior to use.

The 12 mm ( $\frac{1}{2}$  in.) and 19 mm ( $\frac{3}{4}$  in.) maximum size basalt had a bulk specific gravity (saturated surface dry) = 2.64; and absorption (dry) = 0.4 percent. The unit weights (saturated surface dry) for the 12 mm ( $\frac{1}{2}$  in.) and 19 mm ( $\frac{3}{4}$  in.) maximum size aggregates were  $1480 \text{ kg/m}^3$  ( $92.4 \text{ lb/ft}^3$ ) and  $1512 \text{ kg/m}^3$  ( $94.4 \text{ lb/ft}^3$ ), respectively. The 12 mm ( $\frac{1}{2}$  in.) maximum size crushed limestone had a bulk specific gravity (saturated surface dry) = 2.58; and absorption (dry) = 2.7 percent. The unit weight (saturated surface dry) for the 12 mm maximum size aggregate was  $1450 \text{ kg/m}^3$  ( $90.5 \text{ lb/ft}^3$ ).

The water reducer used in the study was a Type A normal-range water reducer

(Master Builders Polyheed 997). The admixture had a specific gravity of 1.27 and contained 47 percent solids by weight. It was used at the rate of 460 ml per 100 kg of cementitious material (7 oz/cwt) for the high-strength test specimens. The high-range water reducer (HRWR) used was a calcium naphthalene sulfonate condensate-based material (Master Builders Rheobuild 1000). The HRWR had a specific gravity of 1.20 and contained 40 percent solids by weight. The quantity of HRWR used varied with each mixture because it was added until the desired workability was attained.

Mixtures were proportioned to limit the number of variables in the study. Cement replacement with 10 percent and 5 percent by weight of silica fume and fly ash, respectively, was kept constant in the high-strength mixtures, as was the total cementitious material content. The water-to-cementitious material ratio varied between 0.24-0.28 for the high-strength mixtures and was kept constant at 0.50 for the normal-strength mixtures. Mixture designs are given in Tables 2.1 and 2.2 for SI and customary units, respectively.

## **2.2 PREPARATION**

Prior to batching, the aggregate moisture content was obtained according to ASTM C 70. The water and aggregate weights were then corrected.

The concrete was mixed in a Lancaster counter-current mixer with a maximum capacity of 0.057 m<sup>3</sup> (2 ft<sup>3</sup>). Prior to batching, the mixer pan was wiped down with water to ensure that all of the mixing water was used to hydrate the cementitious material. All dry materials were placed in the pan and mixed until uniform. For normal-strength concretes, water was added to the dry materials as they were mixing. When needed, water reducer was added until a slump of 7.6 to 10.2 cm (3 to 4 in.) was reached. For high-strength concretes, the water reducer was combined with the mix water prior to addition to the dry materials. The HRWR was then slowly added until a slump of 20 to 24 cm (8 to 9½ in.) was obtained. Concrete was mixed for an additional 3 minutes after all materials had been added. After mixing, prismatic test specimens were placed vertically in 100 x 100 x 350 mm (4 x 4 x 14 in.) steel forms.

The concrete was consolidated in 3 layers, each layer rodded 25 times with a 16 mm ( $\frac{5}{8}$  in.) steel rod. The forms were sealed at the top, and the specimens were stored in a horizontal position to reduce the effects of bleeding and to ensure uniform properties throughout the height of the specimens. Most specimens were removed from the molds at 24 hours. However, due to the retarding effects of HRWR, some specimens did not fully set within the first day and were given an additional 24 hours before they were able to be removed.

Concrete specimens designed to reach a strength of 103 MPa (15,000 psi) were placed in lime saturated water until the time of testing. Lower strength specimens, 28 to 86 MPa (4,000 to 12,500 psi), were placed in a curing room meeting the requirements of ASTM C 31.

Prior to testing, the specimens to be loaded in uniaxial compression were shortened to obtain a length-to-width ratio of 3 to 1 by removing equal portions from each end with a high-speed masonry saw. Fracture test specimens were notched at mid-span to a depth of 25 mm (1 in.) and a width of 5 mm (0.2 in.) with the masonry saw. All specimens were placed back in its original curing environment until the time of testing.

## 2.3 TESTING

A minimum of 2 days prior to testing, the uniaxial compression specimens were capped with a 1.6 mm (1/16 in.) layer of Forney Hi-Cap® capping compound and placed back in the curing environment. The specimens were wrapped in plastic wrap, to assure testing in the moist condition, and were loaded at a rate of 0.14 to 0.34 MPa/sec (20 to 50 psi/sec) as specified by ASTM C 39, using a 180,000 kg (400,000 lb) capacity hydraulic testing machine.

Flexural tests were performed using center-point loading, in accordance with ASTM C 293, using a 180,000 kg (400,000 lb) capacity hydraulic testing machine. The specimens were also wrapped in plastic wrap. When needed, leather shims with

a thickness of 6 mm ( $\frac{1}{4}$  in.) were used to remove gaps in excess of 0.10 mm (0.004 in) between the specimen and the supports. Specimens were loaded at an extreme fiber stress rate of 0.86 to 1.21 MPa/min (125 to 175 psi/min) until failure.

Fracture energy tests were performed using an MTS closed-loop electro-hydraulic testing system. The loading apparatus is shown in Figure 2.1. At the time of test, 2 steel plates, with lips that slipped into the sawed notch, and with dimensions of 25 mm x 76 mm (1 in. x 3 in.), were superglued along each side of the notch located at midspan of the specimen. A clip gage was placed in the closed position between knife edges attached to the steel plates. The gage measured the horizontal displacement at the mouth of the crack (crack mouth opening displacement or CMOD) and was used to control the rate of loading during the test. Linear variable differential transformers (LVDTs) were attached to aluminum bars spanning the length of the specimen (Figure 2.1). The LVDTs were used to measure the deflection of the specimen at mid-span. A data acquisition system, interfaced with a personal computer, was used to record readings from the extensometer, LVDTs, and MTS load cell. Tests lasted between 15 to 60 minutes, depending upon the specimen compressive strength and aggregate type. However, all specimens were loaded to reach the maximum load approximately 30 seconds after the start of the test, as recommended by RILEM (1985).

## **CHAPTER 3**

### **RESULTS**

This chapter describes the results of the compression, flexure, and fracture energy tests. An evaluation of these tests will be presented in Chapter 4. The purpose of these tests is two-fold: (1) to determine the effects of aggregate type, size, and content on the behavior of normal and high-strength concrete, and (2) to determine the relationships between compressive strength, flexural strength, and fracture energy.

#### **3.1 COMPRESSION TEST RESULTS**

A summary of the individual compression tests is presented in Table 3.1. The results show variations in compressive strength among specimens in the same group. Regardless of the type of test, differences exist because concrete is a composite material whose behavior depends on the behavior of its constituent materials. Since no two specimens are alike, it is not surprising that test specimens from the same batch yield different results. Differences in compressive strength for some normal-strength specimens may also be caused by minor chipping of the concrete due to difficulties with the removal of the concrete from the prismatic molds. Differences in strength may also be due to the effects of bleeding. Although the specimens were stored in a horizontal position, some bleeding was clearly evident, especially in the normal-strength specimens. The bleeding manifested itself in the form of excess bleed water on the top corner of the specimen, resulting in a somewhat smaller cross-sectional area at one end. However, since the top and bottom thirds were confined by friction with the loading platens, failure was initiated in the middle third of the specimen, thus reducing the chance that differences in strength were due to bleeding.

##### **3.1.1 EFFECTS OF AGGREGATE TYPE ON COMPRESSIVE STRENGTH**

The high-strength concrete tests show mixed results on the effect of aggregate type on compressive strength. Comparing basalt and limestone mixes with high

aggregate contents, HB-12h.3 and HL-12h.2, tested at 119 days and 111 days, respectively, shows that the basalt mix yields a greater compressive strength than the comparable limestone mix, a difference of 11.4 percent; little of this difference can be attributed to the small difference in test ages. Comparing another pair of basalt and limestone mixes with high aggregate contents, HB-12h.2 and HL-12h.1, tested at ages 149 days and 148 days, respectively, shows that the basalt mix yields a compressive strength of 81.8 MPa (11,870 psi) while the limestone mix yields a compressive strength of 79.6 MPa (11,550 psi), a difference of only 2.6 percent, with the basalt mix again yielding the greater compressive strength. However, comparing a basalt and limestone mix containing low aggregate contents, HB-12l.2 and HL-12l, tested at 117 and 94 days, respectively, shows the *limestone* mix yielding an 11.3 percent greater strength than the basalt mix. The difference in strength would presumably increase if both specimens were tested at 117 days.

For the normal-strength concretes with high aggregate contents, the limestone mix yields an 8.8 percent *higher* compressive strength than the basalt mix. However, since 5-day strengths are only about 60 percent of the 28-day strength, no solid conclusions can be made.

Fracture surfaces provide useful information in the study of the compressive strength of concrete. It has been observed that the fracture of normal-strength concrete coincides with a gradual softening of the specimen. Fracture involves a large number of inclined microcracks located mainly in the middle half of the specimen, leaving the confined ends, which are in contact with the platens, generally unaffected by the cracks. The failure of high-strength concrete is, however, very different from that of normal-strength concrete. After reaching the peak load, fracture of high-strength concrete results in the release of a significant amount of energy which is stored within both the specimen and the testing machine. For relatively flexible testing machines, as used in this study, this energy release results in an explosive failure, with the specimen fracturing into countless pieces. In this case, fracture involves a large number of cracks that tend to propagate nearly parallel to the loading axis.

Aggregate type is a factor in the appearance of fracture surfaces. In normal-

strength concrete, cracks extend through the matrix, bridging between the coarse aggregate particles, leaving a tortuous fracture surface with a considerable amount of branching. In the current study, there was no noticeable fracture of the basalt particles at the fracture surface; however, there was evidence of a few fractured limestone particles. The tortuous path of the limestone fracture surface is not as distinct as that of the basalt, yielding a smoother fracture surface than produced by the basalt. In high-strength concrete, cracks extend through the matrix, similar to that of normal-strength concrete; however, instead of cracks bridging between the coarse aggregate particles, cracks propagate through the particles, resulting in a smooth fracture surface. In the current study, there was noticeable, but not complete, fracture of the basalt aggregate at the surface of the crack. In contrast, *all* of the limestone aggregate was fractured, leaving the smoothest fracture surfaces produced by any of the compressive strength specimens.

### 3.1.2 EFFECTS OF AGGREGATE SIZE ON COMPRESSIVE STRENGTH

The high-strength concrete test results to determine the effect of aggregate size on compressive strength show that concrete with a 12 mm ( $\frac{1}{2}$  in.) maximum size aggregate yields higher compressive strengths than concrete with a 19 mm ( $\frac{3}{4}$  in.) maximum size aggregate, although the difference is not significant. Concrete containing basalt, HB-12h.3 and HB-19h.2, tested at 119 and 116 days, respectively, shows a 3.0 percent increase in compressive strength for the smaller maximum size aggregate. In normal-strength concrete, the 19 mm ( $\frac{3}{4}$  in.) coarse aggregate yields a slightly *higher* compressive strength than the comparable 12 mm ( $\frac{1}{2}$  in.) coarse aggregate (NB-19h and NB-12h). In this case the difference is 7.6 percent. However, as previously mentioned, no solid conclusion can be made based on 5-day strengths.

In comparing the fracture surfaces of the 12 mm ( $\frac{1}{2}$  in.) and 19 mm ( $\frac{3}{4}$  in.) basalt in high-strength concrete, there is no noticeable difference in the appearance or the amount of fractured coarse aggregate particles. The fracture still involves a large number of cracks that propagate parallel to the axis of loading, and extend through the

matrix and a number of the aggregate particles. In normal-strength concrete, however, the fracture surface of the concrete containing 19 mm ( $\frac{3}{4}$  in.) maximum size aggregate shows a more tortuous path, providing a rougher fracture surface than the concrete containing 12 mm ( $\frac{1}{2}$  in.) maximum size aggregate.

### **3.1.3 EFFECTS OF AGGREGATE CONTENT ON COMPRESSIVE STRENGTH**

Test results to determine the effect of aggregate content on compressive strength show that, in high-strength concrete containing basalt, the compressive strength increases with increasing aggregate content. Mixes with high and low basalt coarse aggregate contents, HB-12h.3 and HB-12l.2, tested at 119 and 117 days, respectively, yield compressive strengths of 80.1 MPa (11,620 psi) and 62.5 MPa (9,070 psi), respectively, a difference of 21.9 percent. At higher test ages of 164 and 160 days for the high and low basalt coarse aggregate contents, HB-12h.1 and HB-12l.1, respectively, there is a difference of 2.7 percent in compressive strength, the high aggregate content again yielding higher strengths. In high-strength concrete containing limestone, the difference in compressive strengths is only a fraction of a percent. Thus, aggregate content does not seem to be a factor in high-strength concrete containing the (lower strength) limestone coarse aggregate.

The test results also show that in normal-strength concrete, compressive strength increases with increasing aggregate content for both aggregate types, although the difference in compressive strength between high and low aggregate contents is greater in the basalt mix than the limestone mix. After 5 days, concrete containing a higher basalt coarse aggregate content yields higher compressive strengths than the concrete containing a lower basalt coarse aggregate content, by as much as 9.2 percent; however, concrete with higher limestone coarse aggregate content yields only a 4.2 percent higher compressive strength than the concrete with the lower limestone coarse aggregate content, less than one-half of the difference in basalt mixes.

The fracture surfaces of the concrete containing high and low coarse aggregate



contents are very similar for both the high-strength and normal-strength concretes, where cracks propagate through a number of basalt particles and through all of the limestone particles at high-strengths, and travel around the aggregate particles at normal-strengths.

### **3.2 FLEXURE TEST RESULTS**

The individual flexure tests are summarized in Table 3.2.

The flexure specimens were tested on the same days as the compression specimens from the same group. Thus, the high-strength concrete specimens were tested at ages ranging from 94 to 164 days, while the normal-strength concrete specimens were tested 5 days following casting. To study the effects of aggregate type, size, and content, comparisons are made between concretes tested at approximately the same age. Slight differences in test age may be a factor in the differences in flexural strength for high-strength concrete. Differences in flexural strength of normal-strength concrete may also have been caused by minor chipping of the specimens in several areas due to difficulties with the removal of the concrete from the prismatic molds. Bleeding may also be a factor in the strength of the specimens. However, the reduction in the cross-sectional area at one end due to bleeding, similar to that discussed for compressive specimens, does not affect the effective cross-sectional area at midspan of the test specimen.

#### **3.2.1 EFFECTS OF AGGREGATE TYPE ON FLEXURAL STRENGTH**

The test results for high-strength concrete show that at all ages, concrete containing basalt yields higher flexural strengths than the corresponding concrete containing limestone. For tests at 119 and 111 days, HB-12h.3 and HL-12h.2, the basalt mix yields a flexural strength of 10.2 MPa (1,480 psi), while the limestone mix yields a flexural strength of 8.1 MPa (1,180 psi), a difference of 20.3 percent. Tests conducted at 149 and 148 days, HB-12h.2 and HL-12h.1, show that the basalt mix

yields 19.6 percent greater flexural strength than the limestone mix.

In contrast to the high-strength concrete test results, the results for normal-strength concrete with a high aggregate content show that the basalt mix, NB-12h, yields only 1.8 percent greater flexural strength than the limestone mix, NL-12h; however, the results for concrete containing a low aggregate content show that the basalt mix, NB-12l, yields a 10.5 percent *lower* flexural strength than the limestone mix, NL-12l. These results indicate little effect of aggregate type on the flexural strength of the normal-strength concrete. Differences in strengths may be evident at a later test ages.

The fracture surfaces of the flexural specimens were similar to those of the compression test specimens. In normal-strength concrete, the crack propagated around the coarse aggregate particles, leaving a tortuous fracture surface. In high-strength concrete, the cracks propagated through many of the basalt particles and *all* of the limestone particles, resulting in a relatively smooth fracture surface.

### 3.2.2 EFFECTS OF AGGREGATE SIZE ON FLEXURAL STRENGTH

The test results show little effect of aggregate size on flexural strength. For high-strength concrete containing 19 mm ( $\frac{3}{4}$  in.) aggregate, tested at 137 days, and 12 mm ( $\frac{1}{2}$  in.) aggregate, tested at 149 days, HB-19h.1 and HB-12h.2, the larger aggregate size yielded a flexural strength of 11.2 MPa (1,630 psi) while the smaller aggregate size yielded a flexural strength of 10.9 MPa (1,580 psi), a difference of 3.1 percent. Mixes containing 19 mm ( $\frac{3}{4}$  in.) and 12 mm ( $\frac{1}{2}$  in.) aggregate, HB-19h.2 and HB-12h.3, tested at 116 and 119 days, respectively, yielded flexure strengths of 9.9 MPa (1,430 psi) and 10.2 MPa (1,480 psi), respectively, with the smaller maximum aggregate size producing 3.4 percent higher flexural strength than the larger aggregate.

For normal-strength concrete, NB-19h and NB-12h, the larger aggregate size yielded 3.6 percent greater strength than the comparable smaller aggregate size.

Observations on the effect of aggregate size on the appearance of the fracture surfaces of flexural specimens are similar to observations for compression specimens.

For high-strength concrete, cracks propagate through many, if not all, of the aggregate particles, leaving a relatively smooth fracture surface, independent of aggregate size. However, for normal-strength concrete, cracks propagate around the coarse aggregate particles, leaving a tortuous fracture surface -- more so for the 19 mm ( $\frac{3}{4}$  in.) maximum size aggregate than for the 12 mm ( $\frac{1}{2}$  in.) aggregate.

### 3.2.3 EFFECTS OF AGGREGATE CONTENT ON FLEXURAL STRENGTH

For high-strength concrete, the effects of aggregate content on flexural strength vary with aggregate type. The results for concrete containing basalt show that a higher aggregate content yields higher strengths. The high aggregate content mix, tested at 119 days, and the low aggregate content mix, tested 117 days, HB-12h.3 and HB-12l.2, produced flexural strengths of 10.2 MPa (1,480 psi) and 9.0 MPa (1,310 psi), respectively, a difference of 11.5 percent. Comparisons of high and low aggregate content basalt mixes, HB-12h.1 and HB-12l.1, tested at 164 and 160 days, respectively, produced strengths of 12.8 MPa (1,860 psi) and 11.2 MPa (1,630 psi), a 12.5 percent difference.

Similar observations cannot be made for the concretes containing limestone. Concrete containing a higher limestone aggregate content and concrete containing a lower aggregate content, tested at 111 and 94 days, respectively, HL-12h.2 and HL-12l, produced strengths of 8.1 MPa (1,180 psi) and 8.5 MPa (1,240 psi), a difference in flexural strength of 4.8 percent, with the concrete with the *lower* aggregate content yielding the higher strength.

The tests on normal-strength concrete yielded results that are similar to those of the high-strength concrete. The concrete containing a higher basalt coarse aggregate content, NB-12h, produced 8.6 percent greater strength than the concrete containing the lower basalt coarse aggregate content, NB-12l. However, the concrete containing the higher limestone coarse aggregate content, NL-12h, produced a 2.4 percent *lower* strength than the concrete containing the lower limestone coarse aggregate content, NL-12l.

### 3.3 FRACTURE ENERGY TEST RESULTS

The individual fracture energy results are summarized in Table 3.3.

The procedure for determining the fracture energy will be discussed in the following section, along with the test results comparing the effects of aggregate type, size, and content on fracture energy. For normal-strength concrete, small differences in fracture energy may also have been caused by the chipping described earlier for the compression and flexure specimens. The reduction in the cross-sectional area at one end of the beams due to bleeding, however, did not reduce the effective cross-sectional area at the midspan of the test specimen.

#### 3.3.1 DETERMINATION OF FRACTURE ENERGY

Fracture energy is defined as the amount of energy necessary to create one unit area of a crack. The area of a crack is defined as the projected area on a plane parallel to the main crack direction. Figure 3.1 gives a schematic representation of the area being discussed.

As discussed in Chapter 2, the fracture energy of concrete is determined by means of a three-point bend test on notched beams. The deflection at the center of the beam, as well as the load corresponding to that deflection is recorded. Load-deflection points are then plotted, as shown in Figure 3.1, and the energy,  $W_o$ , represented by the area under the curve, is calculated.

The fracture energy is then calculated by the equation (RILEM 1985, Hillerborg 1985):

$$G_f = (W_o + mg\delta_f) / A \quad (3.1)$$

where:  $W_o$  = area under load vs. displacement curve (m-N or in-lb);  
 $m = m_1 + 2m_2$  (kg or lb/g);  
 $m_1$  = mass of beam between the supports, calculated as the total beam

mass multiplied by  $l/L$ ;

$m_2$  = mass of the part of the loading arrangement which is not attached to the machine, but follows the beam until failure;

$l$  = length of beam between supports (m or in.);

$L$  = total length of beam (m or in.);

$g$  = acceleration due to gravity;

$\delta_f$  = deflection at the final failure of the beam (m or in.);

$A$  = cross-sectional area located at midspan above the notch (m<sup>2</sup> or in<sup>2</sup>).

The term  $mg\delta_f$  in Eq. (3.1) can be explained as follows: During the test, the specimen itself is acted upon not only by the imposed load, but also by the weight of the specimen and the testing equipment attached to it. Consequently, the measured load-deflection curve does not represent the total energy of fracture, and a correction is needed to account for this additional load.

Figure 3.1 shows the measured load-deflection curve, with energy  $W_o$  (top-right). The remaining parts of a hypothetically complete load-deflection curve are shown below the measured curve. The additional load  $P_1$  corresponds to the equivalent load applied by the weight of the specimen ( $\frac{1}{2}m_1g$ ) and the weight of the testing equipment ( $m_2g$ ), which are not included in the original measured load.

The total energy of fracture is:

$$W = W_o + W_1 + W_2 \quad (3.2)$$

where:  $W_1 = P_1 * \delta_f = (\frac{1}{2}m_1 + m_2)g\delta_f = \frac{1}{2}mg\delta_f$

It can be demonstrated that  $W_2$  is approximately equal to  $W_1$  (Hillerborg 1985). Thus, the total energy of fracture is:

$$W = W_o + 2P_1 * \delta_f = W_o + mg\delta_f \quad (3.3)$$

This amount of energy, divided by the projected fracture area, gives the value of  $G_f$ .

Detailed data for each test (peak load,  $W_o$ ,  $\delta_p$ ,  $m_1$ ,  $m_2$ , and  $A$ ) are given in Tables A.1 and A.2 for S.I. and customary units, respectively.

### 3.3.2 EFFECTS OF AGGREGATE TYPE ON FRACTURE ENERGY

For all compressive strengths, concrete containing basalt yields a significantly higher fracture energy than concrete of similar strength containing limestone. Comparing a basalt mix tested at 119 days to a limestone mix tested at 111 days, HB-12h.3 and HL-12h.2, shows that the concrete containing basalt yields a fracture energy of 178 N/m (1.02 lb/in) and that concrete containing limestone yields a fracture energy of 64 N/m (0.36 lb/in), a difference of 64 percent. The compressive strength of the basalt concrete was only 11.5 percent higher than the strength of the limestone concrete. Concrete containing a lower basalt aggregate content and a concrete containing a lower limestone aggregate content, tested at 117 and 94 days, respectively, HB-12l.2 and HL-12l, produced energies of 163 N/m (0.93 lb/in) and 65 N/m (0.37 lb/in), a difference of 60 percent, with the concrete containing basalt yielding the higher energy. The compressive strength of the basalt concrete was 11.3 percent *lower* than the strength of the limestone concrete.

Likewise, comparing normal-strength concretes with high aggregate contents, NB-12h and NL-12h, the basalt mix yields a higher fracture energy than the limestone mix, also with a difference of 64 percent, while the compressive strengths show a difference of just 8.5 percent, with the basalt mix yielding the lower strength. Similar results are also obtained for normal-strength concrete with low aggregate content, NB-12l and NL-12l, with the basalt mix yielding 69 percent higher fracture energy than the comparable limestone mix, for compressive strength differences of 13.3 percent, with the basalt mix yielding the lower strength.

Load-deflection curves for high-strength concrete containing high aggregate contents (Figure 3.2) show a significant difference in peak loads, with the basalt mix having a 37 percent higher peak load and a 53 percent greater final deflection than the

limestone mix. For normal-strength concrete containing a high aggregate content (Figure 3.3), the peak loads for the basalt and limestone mixes differ by only 3.3 percent. However, the final deflection of the basalt mix is again greater than the limestone mix, by 68 percent. For normal-strength concrete containing a low aggregate content (Figure 3.4), the peak load for the basalt mix is just 10.6 percent higher than the peak load for the limestone mix; however, the difference in final deflection is much larger, with the basalt mix having a 78 percent greater deflection than the limestone mix. As shown in Figures 3.2 to 3.4, not only are the peak loads and final deflections smaller for the limestone mix than the basalt mix, the portion of the load-deflection curve following the peak load, the softening branch, is much steeper for the limestone mixes than the basalt mixes. The combination of a smaller peak load, smaller final deflection, and steeper softening branch, results in a lower area under the curve and, thus, a lower fracture energy.

Fracture surfaces for fracture specimens are shown in profile in Figure 3.5. In normal-strength concrete, the crack extends around the coarse aggregate particles, leaving a tortuous fracture surface. Like the compression and flexure specimens, there is no noticeable fracture of the basalt particles at the fracture surface; however, there is evidence of a few fractured limestone particles. In high-strength concrete, the crack extends through both the matrix and the coarse aggregate particles, more so for the limestone than for the basalt, resulting in a smoother fracture surface compared to the normal-strength concrete. Overall, high-strength concrete containing limestone produced the smoothest fracture surface, followed by normal-strength concrete containing limestone, high-strength concrete containing basalt, and lastly, normal-strength concrete containing basalt.

### 3.3.3 EFFECTS OF AGGREGATE SIZE ON FRACTURE ENERGY

Test results on the effects of aggregate size on fracture energy show that in high-strength concrete, 19 mm ( $\frac{3}{4}$  in.) basalt yields somewhat lower fracture energy than 12 mm ( $\frac{1}{2}$  in.) basalt. Tests conducted on concrete containing 19 mm ( $\frac{3}{4}$  in.)

basalt, tested at 116 days, and 12 mm ( $\frac{1}{2}$  in.) basalt, tested at 119 days, HB-19h.2 and HB-12h.3, show that the larger maximum aggregate size yields a fracture energy of 169 N/m (0.97 lb/in), while the smaller maximum aggregate size yields a fracture energy of 178 N/m (1.02 lb/in), a difference of 5.1 percent. The smaller maximum aggregate size produced 3 percent greater compressive strength than the larger maximum aggregate size. For mixes containing 19 mm ( $\frac{3}{4}$  in.) and 12 mm ( $\frac{1}{2}$  in.) basalt, HB-19h.1 and HB-12h.2, tested at 137 and 149 days, respectively, the concrete containing the smaller aggregate size yielded 11 percent greater fracture energy than concrete containing the larger aggregate size. The concrete with the smaller maximum aggregate size was 1 percent stronger in compression than the concrete with the larger maximum aggregate size. A portion of the difference in energy can be attributed to differences in test age.

In contrast to the high-strength concretes, in normal-strength concrete, the larger maximum size aggregate provided an 18 percent greater fracture energy than the smaller maximum size aggregate, NB-19h and NB-12h, a difference of 18 percent, for compressive strength differences of 7.3 percent. The latter results coincide with previous work on the effects of aggregate size on fracture energy (Strange and Bryant 1979, Nallathambi, Karihaloo, and Heaton 1984).

Load-deflection curves for high-strength concrete containing 12 mm ( $\frac{1}{2}$  in.) and 19 mm ( $\frac{3}{4}$  in.) basalt seem to vary with test age. The tests conducted at 116 and 119 days (Figure 3.6) show that the concrete containing the smaller aggregate size yields a higher peak load, a steeper softening branch, and a smaller final deflection (by 11 percent) than concrete containing the larger aggregate size. However, the tests conducted at 137 and 149 days (Figure 3.7) show similar peak loads, then a significantly *larger* final deflection for the concrete containing the *smaller* aggregate size. Load-deflection curves for normal-strength concrete containing 12 mm ( $\frac{1}{2}$  in.) and 19 mm ( $\frac{3}{4}$  in.) basalt (Figure 3.8) show, contrary to high-strength concrete, a 20 percent greater peak load for the *larger* aggregate size and a steeper softening branch for the larger aggregate size. Although the softening branch is steeper for the larger aggregate size, the peak load was significantly greater, thus, yielding a higher fracture



energy.

Regardless of strength, fracture surfaces for concrete containing the 19 mm ( $\frac{3}{4}$  in.) coarse aggregate exhibit a greater surface area than surface for concrete containing the 12 mm ( $\frac{1}{2}$  in.) coarse aggregate due to the more tortuous path of the crack associated with the larger aggregate size.

### 3.3.4 EFFECTS OF AGGREGATE CONTENT ON FRACTURE ENERGY

The test results for the effects of aggregate content on fracture energy are not consistent. For high-strength concrete containing basalt, one set of tests corresponding to high and low aggregate contents, HB-12h.3 and HB-12l.2, conducted at 119 and 117 days, respectively, show an 8.4 percent higher fracture energy for the concrete containing the higher aggregate content. Another set of tests corresponding to high and low aggregate contents, HB-12h.1 and HB-12l.1, conducted at 164 and 160 days, respectively, show a 7.2 percent higher fracture energy in the concrete containing the *lower* aggregate content. However, due to errors during testing, only one fracture test on the concrete containing the lower aggregate content in group HB-12l.1 is valid, thus reducing the strength of the latter observation. Contrary to the results for concrete containing basalt, aggregate content does not seem to be a factor in the high-strength concrete containing limestone. The high and low limestone aggregate contents yielded fracture energies of 64 N/m (0.36 lb/in) and 65 N/m (0.37 lb/in), respectively.

For the normal-strength concrete mixes containing basalt, NB-12h and NB-12l, aggregate content does not seem to be a factor. The high and low basalt aggregate contents yield fracture energies of 185 N/m (1.06 lb/in) and 183 N/m (1.05 lb/in), respectively. However, in concrete containing limestone, NL-12h and NL-12l, concrete containing a higher aggregate content yields 15 percent greater fracture energy than concrete containing a lower aggregate content. However, the results may change at a later test age.

Load-deflection curves comparing high-strength concrete containing basalt aggregate yield variable results at different test ages. Load-deflection curves taken at

119 and 117 days (Figure 3.9) show a much higher peak load corresponding to the higher aggregate content, followed by a steeper softening branch and a smaller final deflection. Although the concrete containing the higher aggregate content has a steeper softening branch and smaller deflection, the peak load is significantly higher than the lower aggregate content peak load, yielding a larger area under the load-deflection curve and, thus, a higher fracture energy. Load-deflection curves taken at 164 and 160 days (Figure 3.10) show similar peak loads and softening branches, which is contrary to the load-deflection curves of Figure 3.9; however, the final deflection is again smaller for the higher aggregate content. In contrast to the high-strength concrete containing basalt, there is virtually no difference in the load-deflection curves of the high-strength concrete containing limestone (Figure 3.11), with high and low aggregate contents yielding similar fracture energies.

Load-deflection curves comparing normal-strength concrete containing basalt with high and low aggregate contents (Figure 3.12) show a somewhat steeper softening branch for the concrete containing the higher aggregate content. This, however, is offset by a higher peak load and final deflection, resulting in virtually equal fracture energies. Load-deflection curves comparing normal-strength concrete containing limestone high and low aggregate contents (Figure 3.13) show a higher peak load and a higher final deflection for the concrete containing the higher aggregate content, resulting in a higher fracture energy.

Fracture surfaces of the concrete containing high and low aggregate contents are similar to the fracture surfaces discussed in the previous section. Differences in fracture surface may have been more noticeable if the differences in aggregate contents had been greater.

### **3.4 FLEXURAL STRENGTH VERSUS COMPRESSIVE STRENGTH**

A significant amount of research has been done on the relationship between compressive strength and flexural strength. A common relationship that has been developed (ACI 363-92) is:

$$\begin{aligned}
 R &= 0.94(f'_c)^{1/2} \text{ MPa} \\
 (21 \text{ MPa} < f'_c < 83 \text{ MPa}); \text{ or} \\
 R &= 11.7(f'_c)^{1/2} \text{ psi} \\
 (3,000 \text{ psi} < f'_c < 12,000 \text{ psi})
 \end{aligned}
 \tag{3.4}$$

where:  $R$  = flexural strength (MPa or psi)

$f'_c$  = compressive strength (MPa or psi)

This relationship, along with the results from the research discussed in this report, is shown in Figure 3.14.

For normal-strength concrete, containing either basalt or limestone, flexural strength is 6 to 11 percent higher than predicted by the relationship given in Eq. 3.4. Since all concrete specimens tested yield approximately the same results, aggregate type, size, and content do not appear to be factors in the relationship between compressive and flexural strength.

For high-strength concrete containing limestone, flexural strength is again only 3 to 8 percent higher than predicted by the relationship given in Eq. 3.4. However, for high-strength concrete containing basalt, flexural strength is 16 to 22 percent higher than predicted by Eq. 3.4. The difference increases at compressive strengths greater than 83 MPa (12,000 psi); however, this is outside of the range of compressive strengths, 21 to 83 MPa (3,000 to 12,000 psi), for which Eq. 3.4 is valid.

### 3.5 FRACTURE ENERGY VERSUS COMPRESSIVE STRENGTH

Fracture energy is compared to compressive strength in Figure 3.15. Unlike the results of flexural strength versus compressive strength, there seems to be no well-defined relationship between compressive strength and fracture energy. Fracture energy increases slightly between normal and high compressive strength concretes containing limestone, but *decreases* between normal and high compressive strength

concretes containing basalt. Fracture energy appears to be more dependent on aggregate type than on compressive strength.

As shown in Figure 3.15, all concrete mixes containing basalt, regardless of compressive strength, yield significantly higher fracture energies than comparable limestone mixes. The difference in fracture energy due to aggregate type is as much as 300 percent. Aggregate size also seems to increase the fracture energy; however, this increase is only noticeable in normal-strength concrete. Aggregate content does not seem to significantly affect the fracture energy of concrete at any strength.

Although strength does not seem to influence fracture energy, the load-deflection curves comparing normal-strength concrete to high-strength concrete (Figures 3.16 to 3.20) share three common characteristics -- high-strength concrete yields a significantly higher peak load, a steeper softening branch, and a significantly lower final deflection than normal-strength concrete.

A comparison of normal to high-strength concrete containing 19 mm ( $\frac{3}{4}$  in.) basalt with a high coarse aggregate content (Figure 3.16) shows that normal-strength concrete yields a 40 percent lower peak load and a 71 percent greater final deflection than high-strength concrete. This is the greatest difference in final deflection between normal and high-strength concrete for comparable mixes.

Comparison of normal to high-strength concrete containing 12 mm ( $\frac{1}{2}$  in.) basalt with a high coarse aggregate content (Figure 3.17) shows that the normal-strength concrete yields a 49 percent lower peak load and a 55 percent greater final deflection than the high-strength concrete. This is the greatest difference in peak loads between normal and high-strength concrete for comparable mixes.

Comparison of normal to high-strength concrete containing 12 mm ( $\frac{1}{2}$  in.) basalt with a low coarse aggregate content (Figure 3.18) shows that the normal-strength concrete yields a 41 percent lower peak load and a 33 percent greater final deflection than high-strength concrete.

Comparison of normal to high-strength concrete containing limestone coarse aggregate with a high aggregate content (Figure 3.19) shows that the normal-strength concrete yields a 25 percent lower peak load and a 38 percent greater final deflection

than high-strength concrete. The difference in peak loads is significantly less than the differences in peak loads in concrete containing basalt coarse aggregate.

The load-deflection curves for the limestone *low* aggregate content mix (Figure 3.20) is similar to that of the limestone high aggregate content mix just discussed, where the normal-strength concrete yields a 33 percent lower peak load; however, the difference in final deflection is only 12 percent, one-third that of the high aggregate content, the smallest difference of all the concrete mixes.

### **3.6 FRACTURE ENERGY VERSUS FLEXURAL STRENGTH**

A comparison of fracture energy versus flexural strength is shown in Figure 3.21. Similar to the results of fracture energy versus compressive strength, there appears to be no relationship between fracture energy and flexural strength. Again, fracture energy seems to be more dependent on aggregate type than on flexural strength. As shown in Figure 3.21, all concrete mixes containing basalt, regardless of flexural strength, yield significantly higher fracture energies than comparable limestone mixes. Aggregate size also seems to increase the fracture energy at lower flexural strengths. Aggregate content does not seem to significantly affect the fracture energy of concrete at any flexural strength.

### **3.7 BENDING STRESS -- FRACTURE TEST VERSUS FLEXURAL STRENGTH**

In the previous section, it has been established that there is not a direct correlation between fracture energy and flexural strength. However, since both fracture energy and flexural strength tests apply similar bending stresses to the specimen, perhaps a relationship can be established between the specimens in the two tests by means of the bending stress. The equation (ASTM C 293-94) used to calculate bending stress using three-point loading is:

$$R = 3PL/2bd^2 \quad (3.5)$$

where:  $R$  = bending stress (MPa or psi)  
 $P$  = peak load (N or lb)  
 $L$  = length of specimen between supports (mm or in.)  
 $b$  = width of specimen at the fracture (mm or in.)  
 $d$  = depth of specimen at the fracture (mm or in.)

The bending stresses for fracture energy and flexure were calculated using the corresponding peak loads and dimensions at the fracture plane. The average bending stresses are summarized in Table 3.4 for the specimens in each group.

As shown in Figure 3.22, there is a close relationship between the peak bending stresses in the fracture and flexure tests. For the specimens tested in this study, the best fit linear equation describing the relationship is:

$$y = 0.6662x + 0.71 \text{ (MPa)} \quad (3.6)$$

where:  $y$  = peak bending stress in fracture tests (MPa)  
 $x$  = flexural strength (MPa)

Thus, unlike the comparisons of fracture energy to compressive and flexural strength, where fracture energy appears to be more dependent on aggregate type than on either strength property, there seems to be a well-defined relationship between the bending strengths obtained in the two tests and, by extension (Figure 3.14), between those strengths and compressive strength.

## CHAPTER 4

### EVALUATION

In this chapter, the results of the compression, flexure, and fracture energy tests discussed in the previous chapter are compared to previous research on the effects of aggregate type, size, and content for normal and high-strength concrete.

#### 4.1 COMPRESSION TEST EVALUATION

As stated previously, concrete is a composite material whose behavior depends on the behavior of its constituent materials. There are numerous factors that affect the compressive strength of concrete. The current discussion is limited to the effects of aggregate type, size, and content on strength; however, other factors, such as water-to-cementitious material ratio and test age also play a part in the compressive strength of concrete.

Perhaps the most critical factor in the compressive strength of concrete is the water-to-cementitious material ratio. It is well known that concrete compressive strength increases with decreasing water-to-cementitious material ratio. At low ratios, there is insufficient space for the hydration products to form; thus, complete hydration is not possible, which leads to self-desiccation. However, complete hydration is not essential to attain a high ultimate strength, and unhydrated cement can be expected to remain indefinitely in pastes made at low water-to-cementitious material ratios.

##### 4.1.1 EFFECTS OF AGGREGATE TYPE

As stated in Chapter 3, the results on the effects of aggregate type on compressive strength are not consistent. Comparing the high-strength basalt and limestone mixes containing a high aggregate content shows that the basalt mix yields higher compressive strengths than the limestone mix. However, comparing high-strength concrete basalt and limestone mixes containing a *low* aggregate content shows that the basalt mix yields *lower* compressive strengths than the limestone mix.

The results for concrete containing high aggregate content are consistent with previous work, where concretes containing basalt typically attain higher compressive strengths than concretes containing limestone. For high-strength concrete with weaker coarse aggregate, such as limestone, cracks pass through the aggregates, since the matrix-aggregate bond is stronger than the tensile strength of the aggregate itself. In this case, the concrete strength may be limited by the aggregate strength. This behavior is observed by the fracture surfaces of the concrete test specimens. It was also explained by Carrasquillo, Slate, and Nilson (1981) by viewing high-strength concrete as a more homogeneous material. When the matrix is more compact and the voids are less in number, there is greater compatibility between the strength and elastic properties of the coarse aggregate and the matrix. These researchers also stated that improved compatibility also lowers the stress at the matrix-aggregate interface, reducing the likelihood of interfacial failure. Thus, the cracks are more likely to propagate through the aggregate. Maher and Darwin (1976, 1977) observed that the bond strength between the interfacial region and aggregate plays a less dominant role in the compressive strength of concrete than generally believed. The lack of sensitivity of bond strength to changes in water-to-cement ratio (Hsu and Slate 1963, Taylor and Broms 1964) provides strong support for the matrix, rather than the interface, as the principal controlling factor in the strength of concrete.

The results for the normal-strength concrete show that the limestone mix yields greater compressive strengths than the basalt mix, however, not by a significant amount. In lower strength concretes, the weakest link almost exclusively occurs within the matrix and at the matrix-aggregate interface, where the mechanism of progressive microcracking consists of mortar cracks bridging between nearby bond cracks. This is evident when observing the fracture surfaces of the normal-strength concrete test specimens, which show cracks propagating around aggregate particles. Therefore, aggregate type does not seem to be as significant a factor in the compressive strength of normal-strength concrete as the strength of the matrix and the matrix-aggregate interface. This coincides with the test results from Ezeldin and Aitcin (1991), who concluded that normal-strength concretes are not greatly affected by the type of coarse



aggregate. In contrast, Ozturan and Cecen (1997) found that concretes containing limestone coarse aggregate produce higher compressive strengths than concrete containing basalt or gravel coarse aggregate, which they state may be due to some interfacial chemical reaction which may improve the bond strength.

#### **4.1.2 EFFECTS OF AGGREGATE SIZE**

The current results on the effects of aggregate size on compressive strength show that concrete containing a smaller maximum aggregate size yields similar compressive strengths to concrete containing a larger maximum aggregate size. These limited observations contradict the majority of previous work which states that a smaller maximum aggregate size yields higher compressive strengths than concrete containing a larger maximum aggregate size.

#### **4.1.3 EFFECTS OF AGGREGATE CONTENT**

The results show that the compressive strengths of the concretes with the higher basalt aggregate contents are somewhat higher than the compressive strengths of the concretes with the lower basalt aggregate contents. However, for concretes containing limestone, aggregate content does not seem to be a factor in compressive strength.

These results are similar to those of previous work performed by Kaplan (1959) who found that at very high-strengths, the compressive strength of concrete is greater than that of mortar, indicating that the presence of basalt or limestone coarse aggregate contributes to the ultimate compressive strength of concrete. However, previous work on the effects of aggregate content on compressive strength (Bayasi and Zhou 1993) have concluded that aggregate content seems to have a relatively negligible effect on the compressive strength of concrete.

In normal-strength concrete, the results show that compressive strength increases with increasing aggregate content for both aggregate types, although the increase is greater for basalt mixes than limestone mixes. These results contradict

previous research which states that at normal-strengths, mortar yields greater compressive strengths than concrete, thus implying that concrete containing a lower aggregate content, which also contains a larger mortar volume, would yield higher compressive strengths than concrete containing a higher aggregate content. Since only 5-day strengths are recorded, the results may differ at later ages.

## **4.2 FLEXURE TEST EVALUATION**

This section addresses the effects of aggregate type, size, and content on flexural strength.

### **4.2.1 EFFECTS OF AGGREGATE TYPE**

As stated in Chapter 3, the results show that high-strength concrete containing basalt yields higher flexural strengths than concrete containing limestone. Previous work by Kaplan (1959) shows that at all ages, flexural strengths for basalt mixes are higher than limestone mixes with the same proportions. Ozturan and Cecen (1997) have also found that flexural strengths for basalt mixes are higher than limestone mixes. However, contrary to these results, Giaccio et al. (1992) stated that aggregate type does not affect flexural strength. It has been noted, though, that flexural strength of basalt is almost twice the value of the flexural strength for limestone. The greater aggregate strength should contribute to the higher flexural strengths observed for concrete containing basalt.

Fracture surfaces for the limestone mixes show that flexural strength is limited by the strength of the rock, since all of the limestone particles were fractured at the surface. However, fracture surfaces for the basalt mixes show that flexural strength is controlled by the strength of the rock *and* the bond strength at the matrix-aggregate interface, since only some of the basalt particles were fractured at the surface.

Contrary to the results for high-strength concrete, normal-strength concrete shows no difference in flexural strength for concrete containing basalt or limestone.

Since only a small amount of particles were fractured at the surface, the flexural strength seems to be limited by the strength of the matrix and the interfacial transition zone, not, however, necessarily by the type of aggregate. Ozturan and Cecen (1997) observed that normal-strength concrete containing limestone yields higher flexural strengths than concrete containing basalt or gravel. They state that it is probably due to better bonding of limestone aggregate particles to the matrix.

#### **4.2.2. EFFECTS OF AGGREGATE SIZE**

The test results show that aggregate size has little effect on the flexural strength of high-strength concrete. Perhaps the effect of aggregate size on flexural strength would be more noticeable with a greater difference in aggregate size. As stated previously, in high-strength concrete, flexural strength is controlled by the strength of the rock *and* the interfacial strength at the matrix aggregate interface. However, studies by Strange and Bryant (1979) and Cook (1989) show that an increase in aggregate size decreases the flexural strength of high-strength concrete. Normal-strength concrete test results also show that aggregate size does not affect the flexural strength of concrete. These results support studies by Walker and Bloem (1960) which show that aggregate size has a negligible effect on flexural strength. Again, flexural strength seems to be limited by the strength of the matrix and the interfacial transition zone, not necessarily the aggregate itself.

#### **4.2.3 EFFECTS OF AGGREGATE CONTENT**

The current results show that high-strength concretes containing higher basalt aggregate contents yield higher flexural strengths than concretes containing low aggregate contents. Bayasi and Zhou (1993) also reported that increases in aggregate content increase flexural strength. They state that aggregates work to arrest cracks when subjected to flexural loads; therefore, an increase in aggregate content increases the capacity of the concrete to arrest cracks.

Contrary to the results of high-strength concrete containing basalt, high-strength concrete containing higher limestone aggregate contents yields slightly lower flexural strengths than concrete containing low aggregate contents. As evident by the smooth fracture surfaces of high-strength concrete containing limestone, the aggregate particles are too weak to arrest flexural cracks, and cracks seem to propagate easily through the limestone particles. Since the particles are relatively weak, an increase in limestone aggregate content has a negligible effect on flexural strength.

The normal-strength concrete results are similar to those of the high-strength concrete, where the concrete containing the high basalt aggregate content yields higher flexural strengths than the concrete containing the low aggregate content; and concrete containing a high limestone aggregate content yields a somewhat lower flexural strength than the concrete containing the low aggregate content. Kaplan (1959) found that concrete yields similar flexural strengths to that of mortar, implying that the presence of coarse aggregate does not affect flexural strengths.

### **4.3 FRACTURE ENERGY TEST EVALUATION**

This section addresses the effects of aggregate type, size, and content on fracture energy.

#### **4.3.1 EFFECTS OF AGGREGATE TYPE**

The test results show that for high compressive strengths, concrete containing basalt yields significantly higher fracture energies than concrete containing limestone.

DiTommaso (1984) observed that microcracks existing in unloaded concrete are more frequently located in the high porosity layer of the interfacial transition zone. When the concrete is loaded, microcracks at the interface start to progress as debonding cracks; at higher loads, the microcracks at the interface start to branch through the matrix; cracks then begin to bridge together, which eventually causes the concrete to fail. However, aggregates work to arrest the cracks that grow through the

matrix. It is evident by the fracture surface of high-strength concrete containing basalt that cracks propagate in a straight path through the matrix, but upon reaching an aggregate particle, the crack is forced to propagate around the particle, thus increasing the crack area, and hence, the fracture energy.

This type of crack propagation is not evident in high-strength concrete containing limestone. Since limestone aggregate is relatively weak, the crack propagates through the coarse aggregate as it does through the matrix, creating a smooth fracture surface where all of the limestone particles are fractured. Since the crack in high-strength concrete containing limestone has a shorter distance to travel (compared to concrete containing basalt), it yields a smaller crack area, and thus, a lower fracture energy.

Normal-strength concrete test results also show that concrete containing basalt yields significantly higher fracture energies than concrete containing limestone. It is also evident by the appearance of the fracture surfaces of normal-strength concrete that basalt aggregate works to arrest cracks, while the limestone aggregate, seen fractured at the surface, does not contribute significantly to the arrest of cracks, and thus, yields lower fracture energies.

#### **4.3.2 EFFECTS OF AGGREGATE SIZE**

The test results show that the high-strength concretes containing the smaller maximum aggregate size yield somewhat higher fracture energies than the concretes containing the larger aggregate. These results are in contrast to other studies that have found an increase in fracture energy with an increase in aggregate size. Strange and Bryant (1979) stated that larger aggregate particles result in a greater increase in crack surface than smaller particles and, thus, require more energy for crack propagation. Perdikaris and Romeo (1995) concluded that, for concrete with larger aggregate, there is a higher degree of matrix-aggregate interlock, resulting in an increase in the energy required for crack propagation. These studies included aggregates with a greater difference in size than used in this study. Thus, the small difference in maximum

aggregate size may contribute to the contradictory results of this study. However, for the high-strength concretes, a significant amount of coarse aggregate particles at the crack surface were fractured. Since the crack propagated through the aggregates, the importance of aggregate size on fracture energy would be diminished.

In normal-strength concrete, however, the larger maximum size aggregate yields a significantly higher fracture energy than the smaller aggregate. As is evident by the fracture surfaces, the crack area is greater in the concrete containing the larger aggregate, since the crack propagated around the particles, thus, yielding higher fracture energies than the concrete containing the smaller aggregate.

#### **4.3.3 EFFECTS OF AGGREGATE CONTENT**

The test results show that for the concrete containing basalt, a higher aggregate content yields higher fracture energies than does a lower aggregate content. Moavenzadeh and Kuguel (1969) stated that the work of fracture increases as aggregate content increases. In concrete, cracks follow a meandering path, tending to go around rather than through the aggregate particles. The meandering path increases the energy required for crack propagation, since the area of the cracked surface is increased.

Results for the high-strength concrete containing limestone, however, show that aggregate content has little effect on fracture energy. It is, again, evident from the fracture surface that the lower strength aggregate particles do not work to arrest crack propagation. Therefore, than increase in aggregate content will have little effect on the fracture energy.

For normal-strength concrete, the results show that aggregate content has little effect on fracture energy for concrete containing basalt (note: this apparent insensitivity may be due to the small number of batches tested); however, high aggregate contents in concrete containing limestone yield higher fracture energies than lower aggregate contents. It has been observed that the interfacial transition zone is the "weak link" in the strength of concrete and plays a dominant role, especially in

normal-strength concrete, where the interfacial transition zone is weaker than in high-strength concrete. It is evident from the fracture surfaces that cracks propagate around the aggregate through the interfacial transition zone and re-enter the matrix between the aggregates. The meandering path increases the energy required for crack propagation, since the area of the cracked surface is increased.

#### **4.4 FLEXURAL STRENGTH - COMPRESSIVE STRENGTH RELATIONSHIP**

The results of this study show that for high compressive strengths, the flexural-to-compressive strength ratio falls between 11 and 14 percent. Kaplan (1959) found that flexural-to-compressive ratios for both basalt and limestone high-strength concretes range from 8 to 11 percent. Cook (1989) also studied the flexural-to-compressive strength ratio for high-strength concrete and found that the ratio is nearly constant, at approximately 12 percent.

The flexural-to-compressive strength ratios for normal-strength concrete are quite different. All of the normal-strength concretes produced strength ratios between 18 and 20 percent. These results are contrary to the study done by Walker and Bloem (1960) who found that for normal compressive strengths, the flexural-to-compressive strength ratio remains constant at 12 percent.

A comparison was also made between the results of this study and the flexural-to-compressive strength relationship given in Eq. 3.4 (Figure 3.14). The test results for all normal-strength concretes and the high-strength concretes containing limestone show slightly higher ratios than given by the relationship. However, flexural tests using center-point loading typically produce somewhat greater flexural strengths than flexure tests using third-point loading, which was the specified test method used in developing the relationship given in Eq. 3.4.

Test results on high-strength concrete containing basalt show significantly higher flexural-to-compressive strength ratios than Eq. 3.4. The high tensile strength of the basalt significantly increases the overall flexural strength, which, thus, increases

the flexural-to-compressive strength ratio values above the relationship given in Equation 3.4.

#### **4.5 FRACTURE ENERGY - COMPRESSIVE STRENGTH RELATIONSHIP**

The test results show no well-defined relationship between compressive strength and fracture energy. Fracture energy seems to be more dependent upon aggregate type than upon compressive strength. The concrete mixes containing limestone yield only slightly higher fracture energies for a two-fold increase in compressive strength. Concrete mixes containing basalt yield higher fracture energies at lower compressive strengths than at higher compressive strengths.

Zhou et al. (1995) studied high-strength concrete containing gravel and limestone and observed a decrease in fracture energy with increasing compressive strength. They concluded that the fracture energy decrease may be due to the improvement in the matrix-aggregate bond which results in cracks developing through aggregate particles rather than passing along the matrix-aggregate interface. Contrary to these results, Gettu, Bazant, and Karr (1990) observed slight increases in fracture energy with significant increases in compressive strength. However, the study was done on high-strength concrete containing gravel, which may yield different results than high-strength concrete containing basalt or limestone. Giaccio, Rocco, and Zerbino (1993) studied the relationship between compressive strength and fracture energy on concretes containing various aggregate types, including basalt and limestone. They concluded that fracture energy increases as concrete compressive strength increases, although the increase in fracture energy is not as great as the increase in strength.

#### **4.6 FRACTURE ENERGY - FLEXURAL STRENGTH RELATIONSHIP**

Like the fracture energy-compressive strength relationship, the test results show no relationship between fracture energy and flexural strength. Again, as with



compressive strength, fracture energy is more dependent upon aggregate type than on flexural strength. Flexural strength seems to be limited by the matrix strength and the strength of the interfacial transition zone, while fracture energy is more dependent upon the strength of the aggregate. If the aggregate is stronger than the interfacial transition zone, the crack will propagate around the aggregate particles, thus increasing the fracture energy; however, if the aggregate is weaker than the interfacial transition zone, the crack will propagate through the aggregate particles, thus decreasing the fracture energy.

#### **4.7 BENDING STRESS – FRACTURE TEST - FLEXURAL STRENGTH**

Test results show a strong correlation between the bending stress in the fracture and flexural strength tests. Ultimately, this correlation can be used to find the relationship between stress and crack tip opening displacement, in order to better understand the material properties of concrete. This close relationship between fracture energy and flexural strength provides a means to determine the peak stress for use in developing the stress - crack width relation for the concrete under study.

## **CHAPTER 5**

### **SUMMARY AND CONCLUSIONS**

#### **5.1 SUMMARY**

The purpose of this investigation is two-fold: (1) to determine the effects of aggregate type, size, and content on the compressive strength, flexural strength, and fracture energy of normal and high-strength concrete, and (2) to determine the relationships between these three measures of materials performance.

The concrete in this study incorporates either crushed basalt or limestone coarse aggregate with sizes of 12 mm ( $\frac{1}{2}$  in.) or 19 mm ( $\frac{3}{4}$  in.), and coarse aggregate contents with aggregate volume factors (ACI 211.1-91) of 0.67 or 0.75. Water-to-cementitious materials ratios range from 0.24 to 0.50. Compressive strengths range from 25 MPa to 97 MPa (3,670 psi to 13,970 psi).

Fifteen batches (5 normal-strength concrete and 10 high-strength concrete) of 9 specimens each were tested (except for HL-12h.1 where only 6 specimens were tested). The results of 45 compression, 45 flexural, and 42 fracture energy tests are reported. Normal-strength concrete was tested at an age of 5 days and high-strength concrete was tested at ages of 94 to 164 days. Specimens were tested in compression and flexural using a 180,000 kg (400,000 lb) capacity hydraulic testing machine. Fracture energy tests were performed using an MTS closed-loop servo-hydraulic testing system.

#### **5.2 CONCLUSIONS**

The following conclusions are based on the findings for the materials used and tests performed in this study:

1. High-strength concrete containing basalt produces slightly higher compressive strengths than high-strength concrete containing limestone, while normal-strength concrete containing basalt yields slightly lower compressive strengths than normal-strength concrete containing limestone.

2. The compressive strength of both normal and high-strength concrete is little affected by aggregate size.
3. High-strength concrete containing basalt and normal-strength concrete containing basalt or limestone yield higher compressive strengths with higher coarse aggregate contents than with lower coarse aggregate contents. The compressive strength of high-strength concrete containing limestone is not affected by aggregate content.
4. High-strength concrete containing basalt yields higher flexural strengths than concrete with similar compressive strength containing limestone. The flexural strength of high-strength concrete containing limestone is limited by the strength of the rock and the matrix. The flexural strength of high-strength concrete containing basalt is controlled by the strength of the rock and the interfacial strength at the matrix-aggregate interface. The flexural strength of normal-strength concrete containing the basalt or limestone used in this study is not affected by aggregate type, and is limited by the matrix strength and the strength of the interfacial transition zone.
5. The flexural strength of normal and high-strength concrete is not affected by aggregate size.
6. Normal and high-strength concretes containing basalt yield higher flexural strengths with higher coarse aggregate contents than with lower coarse aggregate contents.
7. Normal and high-strength concretes containing basalt yield significantly higher fracture energies than concrete containing limestone.
8. The fracture energy of high-strength concrete decreases with an increase in aggregate size, while the fracture energy of normal-strength concrete increases with an increase in aggregate size.
9. High-strength concrete containing basalt and normal-strength concrete containing limestone yield higher fracture energies with higher coarse aggregate contents than with lower coarse aggregate contents. The fracture energy of high-strength concrete containing limestone and normal-strength

concrete containing basalt is not affected by aggregate content.

10. The flexural-to-compressive strength ratio for high-strength concrete and normal-strength concrete range from 9 to 12 percent and 18 to 20 percent, respectively, in this current study.
11. There is no well-defined relationship between fracture energy and compressive strength, or between fracture energy and flexural strength.
12. There is a close relationship between the peak bending stresses obtained in the flexure and fracture tests.

### 5.3 FUTURE WORK

Although this study provides insight into the effects of aggregate type, size, and content in normal and high-strength concrete, a number of important questions cannot be answered with the available data. Of particular interest are the effects of aggregate size on the compressive strength, flexural strength, and fracture energy of concrete containing limestone. Tests need to be conducted to determine if differences in aggregate size affect concrete containing limestone as it affects concrete containing basalt.

The test results analyzed in this study are for concrete compressive strengths ranging from 25 to 30 MPa (3,670 to 4,430 psi) and from 62 to 96 MPa (9,070 to 13,970 psi). To obtain a complete understanding of the effects of aggregate type, size, and content, tests are required for compressive strengths spanning between the strength ranges, and also at later test ages for normal-strength concretes and earlier test ages for high-strength concretes .

Another aspect of the current study that needs further examination is the relative influence of (1) a larger maximum aggregate size and (2) a much lower coarse aggregate content for both normal and high-strength concretes.

Finally, a microscopic analysis of the concrete matrix and interfacial transition zone is needed to develop a complete understanding of the effects of aggregate on concrete. Only through a full understanding of the response of concrete under general

loading can the behavior of this important construction material be understood.

## REFERENCES

ACI Committee 211. (1991) "Standard Practice for Selecting Proportions for Normal, Heavyweight, and Mass Concrete (ACI 211.1-91)," ACI Manual of Concrete Practice, 1997 Edition, Part 1, Farmington Hills, MI.

ACI Committee 363. (1992) "State-of-the-Art Report on High-Strength Concrete (ACI 363R-92)," ACI Manual of Concrete Practice, 1997 Edition, Part 1, Farmington Hills, MI.

Bayasi, Z. and Zhou, J. (1993) "Properties of Silica Fume Concrete and Mortar," *ACI Materials Journal*, V. 90, No. 4, July-August, pp. 349-356.

Bentur, A. and Mindess, S. (1986) "The Effect of Concrete Strength on Crack Patterns," *Cement and Concrete Research*, V. 16, No. 1, January, pp. 59-66.

Bloem, D. L. and Gaynor, R. D. (1963) "Effects of Aggregate Properties on Strength of Concrete," *ACI Journal, Proceedings* V. 60, No. 10, October, pp. 1429-1456.

Carrasquillo, R. L., Nilson, A. H., and Slate, F. O. (1981) "Properties of High-Strength Concrete Subject to Short-Term Loads," *ACI Journal, Proceedings* V. 78, No. 3, May-June, pp. 171-178.

Carrasquillo, R. L., Slate, F. O., and Nilson, A. H. (1981) "Microcracking and Behavior of High-Strength Concrete Subject to Short-Term Loading," *ACI Journal, Proceedings* V. 78, No. 3, May-June, pp. 179-186.

Cook, J. E. (1989) "10,000 psi Concrete," *Concrete International*, October, pp. 67-75.

Cordon, W. A. and Gillespie, H. A. (1963) "Variables in Concrete Aggregates and Portland Cement Paste Which Influence the Strength of Concrete," *ACI Journal, Proceedings* V. 60, No. 8, August, pp. 1029-1052.

Darwin, D., Tholen, M. L., Idun, E. K., and Zuo, J. (1995) "Splice Strength of High Relative Rib Area Reinforcing Bars," *SL Report* No. 95-3, University of Kansas, May.

Darwin, D. (1995) "The Interfacial Transition Zone: Direct Evidence on Compressive Response," *Material Research Society Symposium Proceedings*, V. 370, pp. 419-427.

DiTommaso, A. (1984) "Evaluation of Concrete Fracture," *Fracture Mechanics of Concrete: Material Characterization and Testing*, Eds. A. Carpinteri and A. R. Ingraffea, Martinus Nijhoff Publishers, Boston, pp. 31-65.

Ezeldin, A. S. and Aitcin, P.-C. (1991) "Effect of Coarse Aggregate on the Behavior of Normal and High-Strength Concretes," *Cement, Concrete, and Aggregates*, CCAGDP, V. 13, No. 2, pp. 121-124.

Gettu, R., Bazant, Z. P., and Karr, M. E. (1990) "Fracture Properties and Brittleness of High-Strength Concrete," *ACI Materials Journal*, V. 87, No. 6, November-December, pp. 608-617.

Gettu, R. and Shah, S. P. (1994) "Fracture Mechanics", Chap. 6, *High Performance Concrete: Properties and Applications*, Shah, S.P. and Ahmad, S.H., Great Britain, pp. 193-212.

Giaccio, G., Rocco, C., Violini, D., Zappitelli, J., and Zerbino, R. (1992) "High-Strength Concretes Incorporating Different Coarse Aggregates," *ACI Materials Journal*, V. 89, No. 3, May-June, pp. 242-246.

Giaccio, G., Rocco, C., and Zerbino, R. (1993) "The Fracture Energy ( $G_F$ ) of High-Strength Concretes," *Materials and Structures*, V. 26, No. 161, August-September, pp. 381-386.

Hillerborg, A. (1985) "The Theoretical Basis of a Method to Determine the Fracture Energy  $G_F$  of Concrete," *Materials and Structures*, V. 18, No. 106, pp. 291-296.

Hsu, T. T. C. and Slate, F. O. (1963) "Tensile Bond Strength Between Aggregate and Cement Paste or Mortar," *ACI Journal, Proceedings* V. 60, No. 4, April, pp. 465-486.

Kaplan, M. F. (1959) "Flexural and Compressive Strength of Concrete as Affected by the Properties of Coarse Aggregate," *ACI Journal, Proceedings* V. 30, No. 11, pp. 1193-1208.

Maher, A. and Darwin, D. (1976) "A Finite Element Model to Study the Microscopic Behavior of Plain Concrete," *SL Report* No. 76-02, University of Kansas, November.

Maher, A. and Darwin, D. (1977) "Microscopic Finite Element Model of Concrete," *Proceedings, First International Conference on Mathematical Modeling*, St. Louis, Vol. III, pp. 1705-1714.

Mindess, S. (1995) "Mechanical Properties of the Interfacial Transition Zone: A Review," *Interface Fracture and Bond*, Eds. O. Buyukozturk and M. Wecharatana, ACI SP-156, American Concrete Institute, Detroit, MI, pp. 67-102.

Moavenzadeh, F. and Kuguel, R. (1969) "Fracture of Concrete," *Journal of Materials*, JMLSA, V. 4, No. 3, pp. 497-519.

Nallathambi, P., Karihaloo, B. L., and Heaton, B. S. (1984) "Effect of Specimen and Crack Sizes, Water/Cement Ratio and Coarse Aggregate Texture upon Fracture Toughness of Concrete," *Magazine of Concrete Research*, V. 36, No. 129, pp. 227-236.

Ozturan, T. and Cecen, C. (1997) "Effect of Coarse Aggregate Type on Mechanical Properties of Concretes with Different Strengths," *Cement and Concrete Research*, V. 27, No. 2, January, pp. 165-170.

Perdikaris, P. C. and Romeo, A. (1995) "Size Effect on the Fracture Energy of Concrete and Stability Issues in 3-Point Bending Fracture Toughness Testing," *ACI Materials Journal*, V. 92, No. 5, September-October, pp. 483-496.

RILEM, 1985-TC 50-FMC, Fracture Mechanics of Concrete, "Determination of the Fracture Energy of Mortar and Concrete by Means of Three-Point Bend Tests on Notched Beams," RILEM Recommendation, *Materials and Structures*, V. 18, No. 16, pp. 287-290.

Ruiz, W. M. (1966) "Effect of Volume of Aggregate on the Elastic and Inelastic Properties of Concrete," M.S. Thesis, Cornell University, January.

Strange, P. C. and Bryant, A. H. (1979) "The Role of Aggregate in the Fracture of Concrete," *Journal of Materials Science*, V. 14, No. 8, pp. 1863-1868.

Taylor, M. A. and Broms, B. B. (1964) "Shear Bond Strength Between Coarse Aggregate and Cement Paste or Mortar," *ACI Journal, Proceedings* V. 61, No. 8, August, pp. 939-957.

Walker, S. and Bloem, D. L. (1960) "Effects of Aggregate Size on Properties of Concrete," *ACI Journal, Proceedings* V. 57, No. 3, September, pp. 283-298.

Xie, J., Elwi, A. E., and MacGregor, J. G. (1995) "Mechanical Properties of Three High-Strength Concretes Containing Silica Fume," *ACI Materials Journal*, V. 92, No. 2, March-April, pp. 135-145.

Zhou, F. P., Barr, B. I. G., and Lydon, F. D. (1995) "Fracture Properties of High-Strength Concrete with Varying Silica Fume Content and Aggregates," *Cement and Concrete Research*, V. 25, No. 3, pp. 543-552.



**Table 2.1**  
**Concrete Mix Proportions**  
**(S.I. Units)**

<b>Group+</b>	<b>w/cm*</b>	<b>Water**</b> (kg/m <sup>3</sup> )	<b>Cement</b> (kg/m <sup>3</sup> )	<b>Silica***</b> (kg/m <sup>3</sup> )	<b>Fly Ash</b> (kg/m <sup>3</sup> )	<b>Type F</b> (L/m <sup>3</sup> )	<b>Type A</b> (L/m <sup>3</sup> )	<b>Rock</b> (kg/m <sup>3</sup> )	<b>Sand</b> (kg/m <sup>3</sup> )	<b>Unit Wt.</b> (kg/m <sup>3</sup> )	<b>Slump</b> (mm)	<b>Test Age</b> (days)
<b>HB-19h.1</b>	0.26	127	411	49	24	13.2	2.1	1105	714	2439	230	137
<b>HB-19h.2</b>	0.26	125	411	49	24	11.0	2.1	1098	714	2427	240	116
<b>HB-12h.1</b>	0.24	119	412	49	24	14.4	2.1	1102	743	2458	230	164
<b>HB-12h.2</b>	0.26	125	410	48	24	24.2	2.1	1096	739	2456	240	149
<b>HB-12h.3</b>	0.28	137	412	49	24	26.6	2.1	1101	714	2451	230	119
<b>HB-12l.1</b>	0.28	133	407	48	24	36.6	2.1	986	846	2463	230	160
<b>HB-12l.2</b>	0.27	133	413	49	24	21.1	2.1	985	824	2439	240	117
<b>HL-12h.1</b>	0.26	125	410	48	24	10.5	2.4	1074	716	2403	240	148
<b>HL-12h.2</b>	0.26	127	411	49	24	11.6	2.4	1071	721	2410	240	111
<b>HL-12l</b>	0.27	133	413	49	24	19.9	2.4	964	829	2423	220	94
<b>NB-19h</b>	0.50	164	327	0	0	0	0	1105	775	2371	100	5
<b>NB-12h</b>	0.50	164	327	0	0	0	0	1105	773	2368	80	5
<b>NB-12l</b>	0.50	164	327	0	0	0	0.7	994	885	2371	80	5
<b>NL-12h</b>	0.50	164	327	0	0	0	0.7	1090	765	2345	100	5
<b>NL-12l</b>	0.50	164	327	0	0	0	1.0	973	883	2347	100	5

+ H = high-strength concrete

N = normal-strength concrete

B = basalt aggregate

L = limestone aggregate

12 = 12 mm (1/2 in.) maximum size aggregate

19 = 19 mm (3/4 in.) maximum size aggregate

h = high aggregate content

l = low aggregate content

.# = batch number

\* Water-to-cementitious material ratio

\*\* Water content includes amount of water in Type A and Type F admixtures.

\*\*\* Condensed silica fume

**Table 2.2**  
**Concrete Mix Proportions**  
**(Customary Units)**

<b>Group+</b>	<b>w/cm*</b>	<b>Water** (lb/yd3)</b>	<b>Cement (lb/yd3)</b>	<b>Silica*** (lb/yd3)</b>	<b>Fly Ash (lb/yd3)</b>	<b>Type F (oz/yd3)</b>	<b>Type A (oz/yd3)</b>	<b>Rock (lb/yd3)</b>	<b>Sand (lb/yd3)</b>	<b>Unit Wt. (lb/ft3)</b>	<b>Slump (in.)</b>	<b>Test Age (days)</b>
HB-19h.1	0.26	213	692	82	41	356	57	1859	1201	151.9	9.00	137
HB-19h.2	0.26	211	691	82	41	297	56	1847	1200	151.2	9.50	116
HB-12h.1	0.24	200	693	82	41	387	57	1854	1250	153.1	9.00	164
HB-12h.2	0.26	211	690	81	41	651	56	1844	1243	153.0	9.50	149
HB-12h.3	0.28	231	693	82	41	714	57	1852	1201	152.7	9.00	119
HB-12l.1	0.28	224	685	81	40	985	56	1659	1423	153.4	9.00	160
HB-12l.2	0.27	224	694	82	41	566	57	1656	1385	151.9	9.50	117
HL-12h.1	0.26	210	690	81	41	282	65	1806	1204	149.7	9.50	148
HL-12h.2	0.26	213	692	82	41	312	65	1801	1212	150.1	9.50	111
HL-12l	0.27	223	694	82	41	536	65	1622	1394	150.9	8.50	94
NB-19h	0.50	275	550	0	0	0	0	1859	1303	147.7	3.75	5
NB-12h	0.50	275	550	0	0	0	0	1858	1300	147.5	3.25	5
NB-12l	0.50	276	550	0	0	0	20	1672	1489	147.7	3.00	5
NL-12h	0.50	276	550	0	0	0	18	1833	1287	146.1	3.75	5
NL-12l	0.50	276	550	0	0	0	27	1637	1485	146.2	4.00	5

+ H = high-strength concrete  
N = normal-strength concrete  
B = basalt aggregate  
L = limestone aggregate  
12 = 12 mm (1/2 in.) maximum size aggregate  
19 = 19 mm (3/4 in.) maximum size aggregate  
h = high aggregate content  
l = low aggregate content  
.# = batch number

\* Water-to-cementitious material ratio  
\*\* Water content includes amount of water in Type A and Type F admixtures.  
\*\*\* Condensed silica fume

**Table 3.1**  
**Compression Test Results**

<u>Group*</u>	<u>f<sub>c</sub> (1)</u> (MPa)	<u>f<sub>c</sub> (2)</u> (MPa)	<u>f<sub>c</sub> (3)</u> (MPa)	<u>f<sub>c</sub> (avg)</u> (MPa)	<u>Test Age</u> (days)	<u>Group*</u>	<u>f<sub>c</sub> (1)</u> (psi)	<u>f<sub>c</sub> (2)</u> (psi)	<u>f<sub>c</sub> (3)</u> (psi)	<u>f<sub>c</sub> (avg)</u> (psi)
HB-19h.1	82.7	81.5	78.3	80.8	137	HB-19h.1	12,000	11,820	11,350	11,720
HB-19h.2	79.5	76.7	76.9	77.7	116	HB-19h.2	11,530	11,130	11,160	11,270
HB-12h.1	92.6	93.0	103.4	96.3	164	HB-12h.1	13,430	13,490	14,990	13,970
HB-12h.2	81.9	84.5	79.1	81.8	149	HB-12h.2	11,880	12,250	11,470	11,870
HB-12h.3	80.6	80.8	78.9	80.1	119	HB-12h.3	11,690	11,720	11,440	11,620
HB-12l.1	93.1	94.3	x	93.7	160	HB-12l.1	13,500	13,680	x	13,590
HB-12l.2	60.4	66.1	61.2	62.5	117	HB-12l.2	8,760	9,580	8,880	9,070
HL-12h.1	80.2	82.3	76.4	79.6	148	HL-12h.1	11,630	11,940	11,080	11,550
HL-12h.2	74.2	67.2	71.4	70.9	111	HL-12h.2	10,760	9,740	10,360	10,290
HL-12l	71.6	71.2	68.8	70.5	94	HL-12l	10,380	10,330	9,980	10,230
NB-19h	29.6	29.4	31.4	30.1	5	NB-19h	4,300	4,260	4,560	4,370
NB-12h	27.6	27.6	28.3	27.9	5	NB-12h	4,010	4,010	4,100	4,040
NB-12l	24.1	26.9	25.0	25.3	5	NB-12l	3,500	3,900	3,620	3,670
NL-12h	30.3	30.5	30.7	30.5	5	NL-12h	4,400	4,430	4,450	4,430
NL-12l	29.7	29.2	28.8	29.2	5	NL-12l	4,310	4,240	4,170	4,240

55

<u>*Concrete Strength</u>	<u>Aggregate Type</u>	<u>Aggregate Size</u>	<u>Aggregate Content</u>
H = high N = normal	B = basalt L = limestone	12 = 12 mm (1/2 in.) 19 = 19 mm (3/4 in.)	h = high l = low

**Table 3.2**  
**Flexure Test Results**

<u>Group*</u>	<u>R (1)</u> (MPa)	<u>R (2)</u> (MPa)	<u>R (3)</u> (MPa)	<u>R (avg)</u> (MPa)	<u>Test Age</u> (days)	<u>Group*</u>	<u>R (1)</u> (psi)	<u>R (2)</u> (psi)	<u>R (3)</u> (psi)	<u>R (avg)</u> (psi)
HB-19h.1	10.3	12.1	x	11.2	137	HB-19h.1	1,490	1,760	x	1,630
HB-19h.2	10.2	9.3	10.1	9.9	116	HB-19h.2	1,480	1,350	1,460	1,430
HB-12h.1	13.0	12.6	13.0	12.8	164	HB-12h.1	1,880	1,830	1,880	1,860
HB-12h.2	11.1	10.1	11.4	10.9	149	HB-12h.2	1,610	1,470	1,650	1,580
HB-12h.3	10.1	10.5	10.0	10.2	119	HB-12h.3	1,460	1,520	1,450	1,480
HB-12l.1	10.9	11.5	x	11.2	160	HB-12l.1	1,580	1,670	x	1,630
HB-12l.2	9.0	8.8	9.2	9.0	117	HB-12l.2	1,310	1,270	1,340	1,310
HL-12h.1	8.4	8.9	8.9	8.8	148	HL-12h.1	1,220	1,290	1,290	1,270
HL-12h.2	7.9	8.3	8.1	8.1	111	HL-12h.2	1,150	1,200	1,180	1,180
HL-12l	8.1	9.0	8.5	8.5	94	HL-12l	1,170	1,310	1,230	1,240
NB-19h	5.6	5.7	6.1	5.8	5	NB-19h	810	820	890	840
NB-12h	5.4	5.7	5.6	5.6	5	NB-12h	790	820	810	810
NB-12l	5.8	4.8	4.8	5.1	5	NB-12l	840	700	690	740
NL-12h	5.7	5.4	5.5	5.5	5	NL-12h	820	790	800	800
NL-12l	5.7	5.7	5.7	5.7	5	NL-12l	820	820	820	820

58

<u>*Concrete</u> <u>Strength</u>	<u>Aggregate</u> <u>Type</u>	<u>Aggregate</u> <u>Size</u>	<u>Aggregate</u> <u>Content</u>
H = high N = normal	B = basalt L = limestone	12 = 12 mm (1/2 in.) 19 = 19 mm (3/4 in.)	h = high l = low

**Table 3.3**  
**Fracture Energy Test Results**

<u>Group*</u>	<u>Gf (1)</u> (N/m)	<u>Gf (2)</u> (N/m)	<u>Gf (3)</u> (N/m)	<u>Gf (avg)</u> (N/m)	<u>Test Age</u> (days)	<u>Group*</u>	<u>Gf (1)</u> (in/lb)	<u>Gf (2)</u> (in/lb)	<u>Gf (3)</u> (in/lb)	<u>Gf (avg)</u> (in/lb)
HB-19h.1	136	137	187	154	137	HB-19h.1	0.78	0.78	1.07	0.88
HB-19h.2	215	140	152	169	116	HB-19h.2	1.23	0.80	0.87	0.97
HB-12h.1	148	164	151	154	164	HB-12h.1	0.84	0.94	0.86	0.88
HB-12h.2	169	194	151	172	149	HB-12h.2	0.97	1.11	0.86	0.98
HB-12h.3	173	206	155	178	119	HB-12h.3	0.99	1.18	0.89	1.02
HB-12l.1	167	x	x	167	160	HB-12l.1	0.95	x	x	0.95
HB-12l.2	158	203	127	163	117	HB-12l.2	0.90	1.16	0.73	0.93
HL-12h.1	x	x	x	x	148	HL-12h.1	x	x	x	x
HL-12h.2	69	63	59	64	111	HL-12h.2	0.39	0.36	0.34	0.36
HL-12l	68	69	59	65	94	HL-12l	0.39	0.39	0.34	0.37
NB-19h	230	220	227	226	5	NB-19h	1.31	1.26	1.30	1.29
NB-12h	198	164	193	185	5	NB-12h	1.13	0.94	1.10	1.06
NB-12l	177	184	177	183	5	NB-12l	1.01	1.05	1.01	1.05
NL-12h	70	67	60	66	5	NL-12h	0.40	0.38	0.35	0.37
NL-12l	53	48	66	56	5	NL-12l	0.31	0.27	0.38	0.32

57

<u>*Concrete</u> <u>Strength</u>	<u>Aggregate</u> <u>Type</u>	<u>Aggregate</u> <u>Size</u>	<u>Aggregate</u> <u>Content</u>
H = high N = normal	B = basalt L = limestone	12 = 12 mm (1/2 in.) 19 = 19 mm (3/4 in.)	h = high l = low

**Table 3.4**  
**Bending Stress Results**

<u>Group*</u>	<u>Stress (MPa)</u> Flexure	<u>Stress (MPa)</u> Fracture Test	<u>Test Age</u> (days)	<u>Group*</u>	<u>Stress (psi)</u> Flexure	<u>Stress (psi)</u> Fracture Test
HB-19h.1	11.2	8.0	137	HB-19h.1	1,630	1,160
HB-19h.2	9.9	7.6	116	HB-19h.2	1,430	1,110
HB-12h.1	12.8	8.6	164	HB-12h.1	1,860	1,250
HB-12h.2	10.9	8.2	149	HB-12h.2	1,580	1,190
HB-12h.3	10.2	8.0	119	HB-12h.3	1,480	1,160
HB-12l.1	11.2	8.0	160	HB-12l.1	1,630	1,150
HB-12l.2	8.8	7.1	117	HB-12l.2	1,310	1,040
HL-12h.2	8.1	5.7	111	HL-12h.2	1,180	820
HL-12l	8.5	5.8	94	HL-12l	1,240	840
NB-19h	5.8	5.1	5	NB-19h	840	730
NB-12h	5.5	4.0	5	NB-12h	810	590
NB-12l	5.1	4.2	5	NB-12l	740	610
NL-12h	5.5	4.2	5	NL-12h	800	610
NL-12l	5.7	3.8	5	NL-12l	820	550

*Concrete Strength	Aggregate Type	Aggregate Size	Aggregate Content
H = high N = normal	B = basalt L = limestone	12 = 12 mm (1/2 in.) 19 = 19 mm (3/4 in.)	h = high l = low

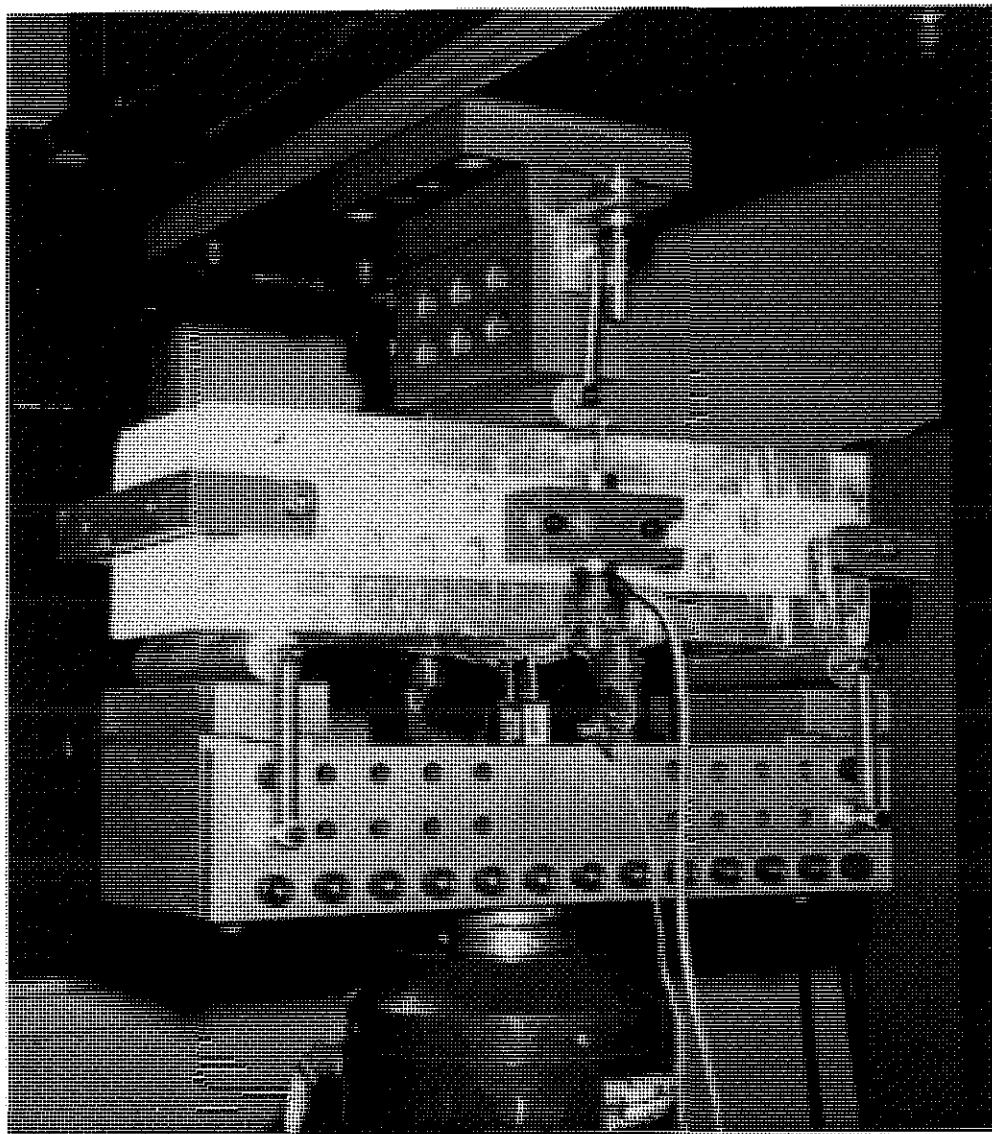


Figure 2.1 Fracture energy test performed using an MTS closed-loop electro-hydraulic testing system.

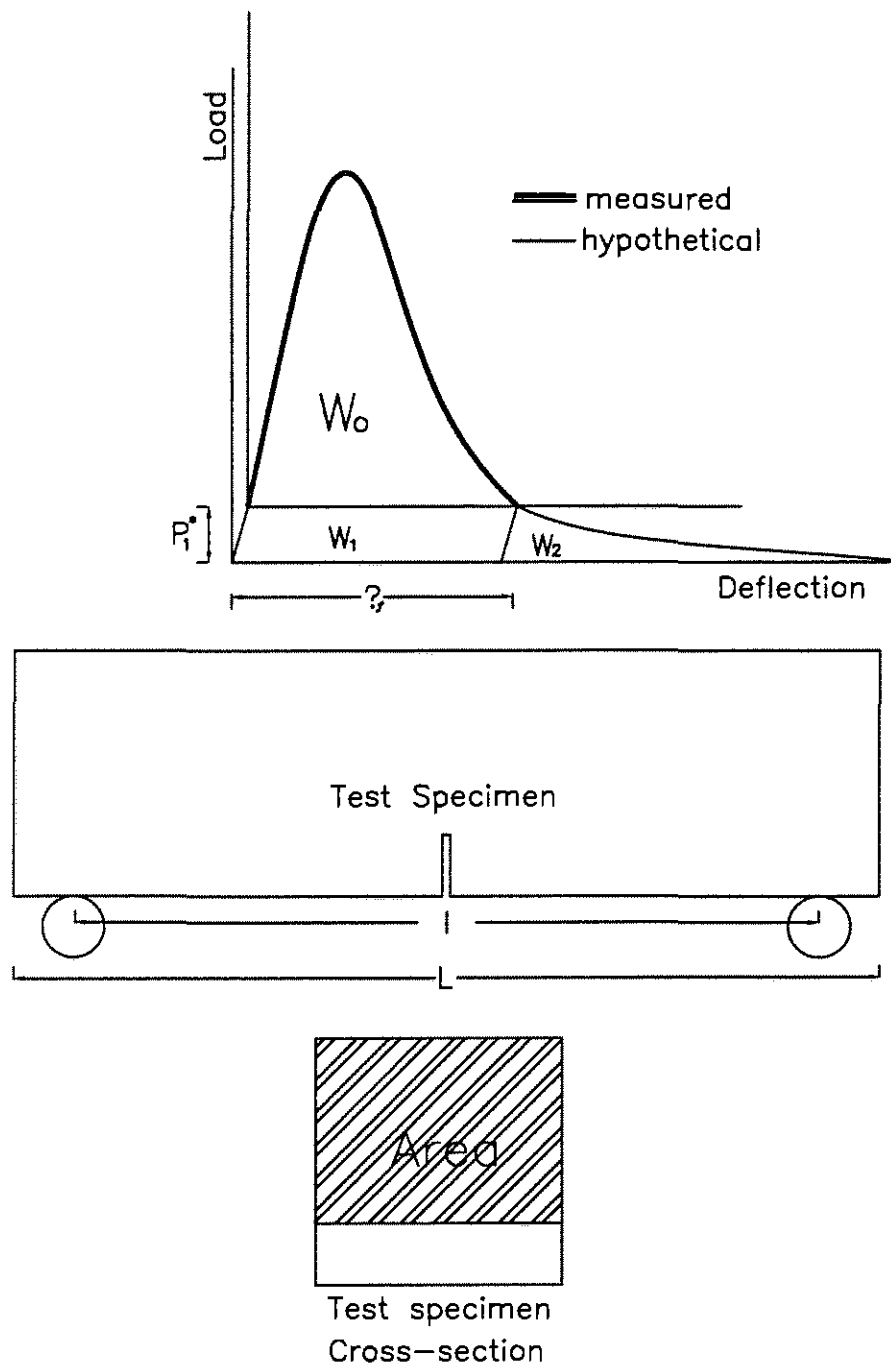


Figure 3.1 Schematic representation of fracture energy test specimen.  
 $W_0$  = area under load-deflection curve;  
 $l$  = length of specimen between the supports;  
 $L$  = length of the total specimen.



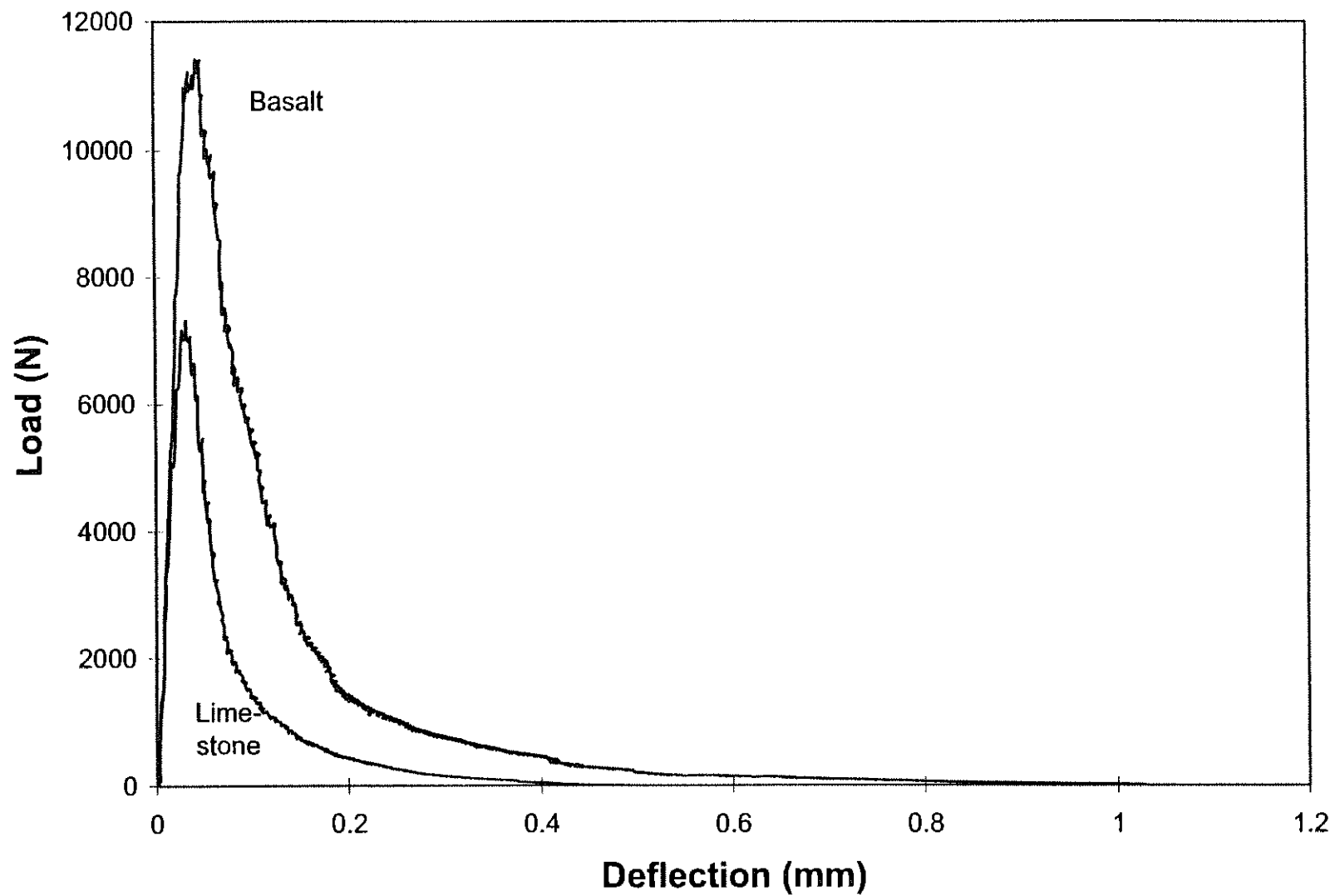


Figure 3.2 Fracture specimen load-deflection curves for basalt and limestone high-strength concretes - high aggregate content. (HB-12h.3 and HL-12h.2)

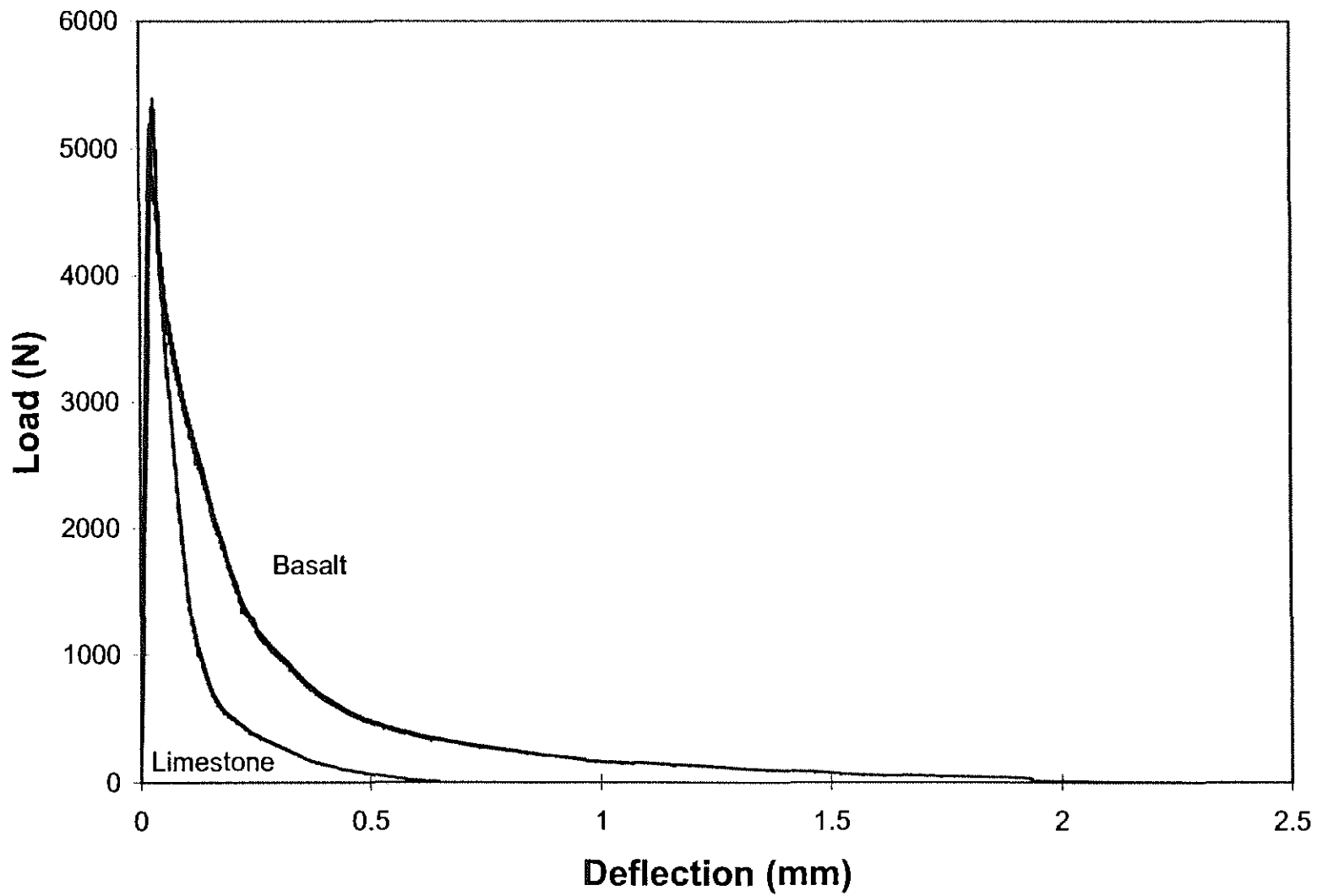


Figure 3.3 Fracture specimen load-deflection curves for basalt and limestone normal-strength concretes -- high aggregate content. (NB-12h and NL-12h)

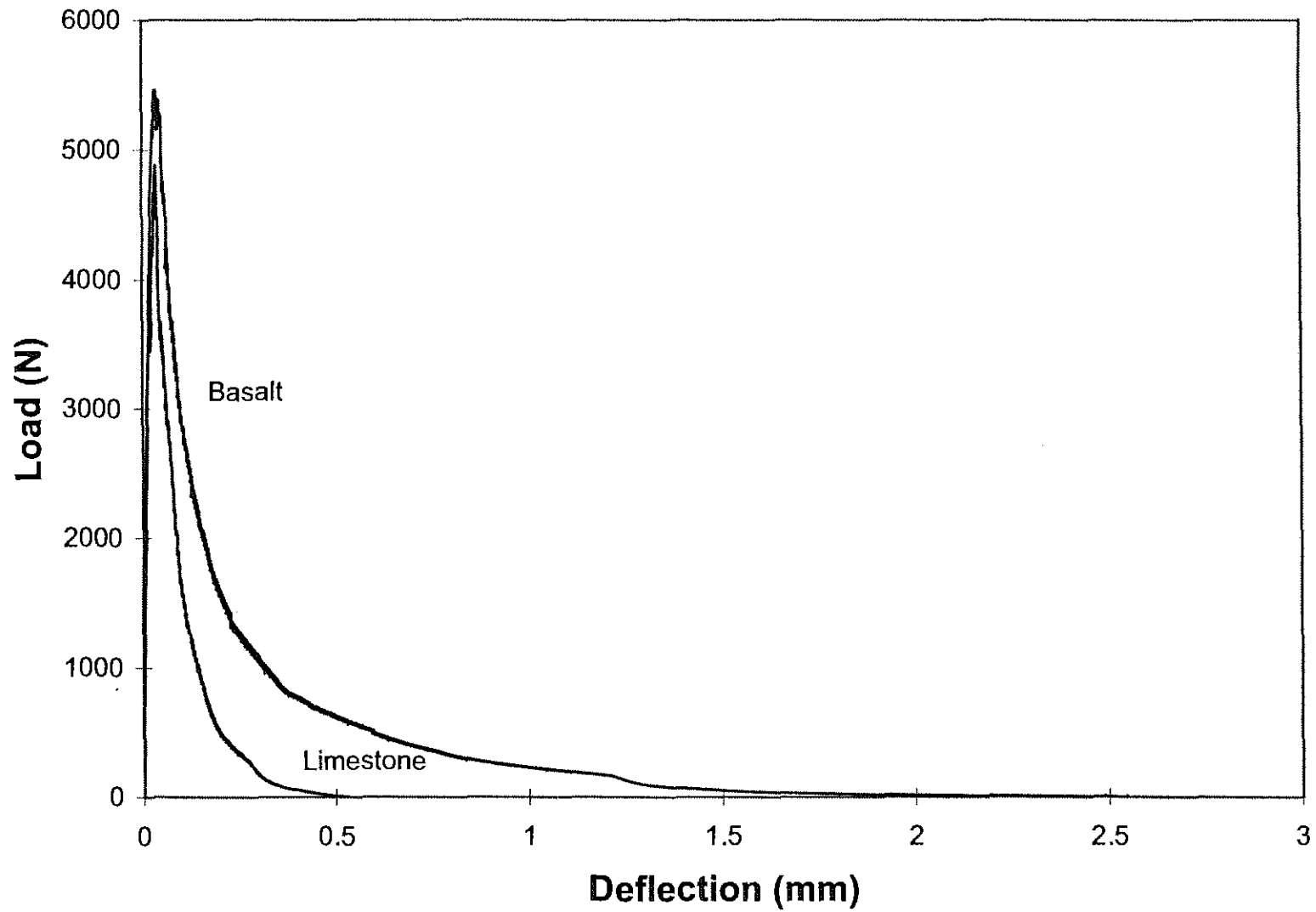


Figure 3.4 Fracture specimen load-deflection curves for basalt and limestone normal-strength concretes -- low aggregate content. (NB-12I and NL-12I)

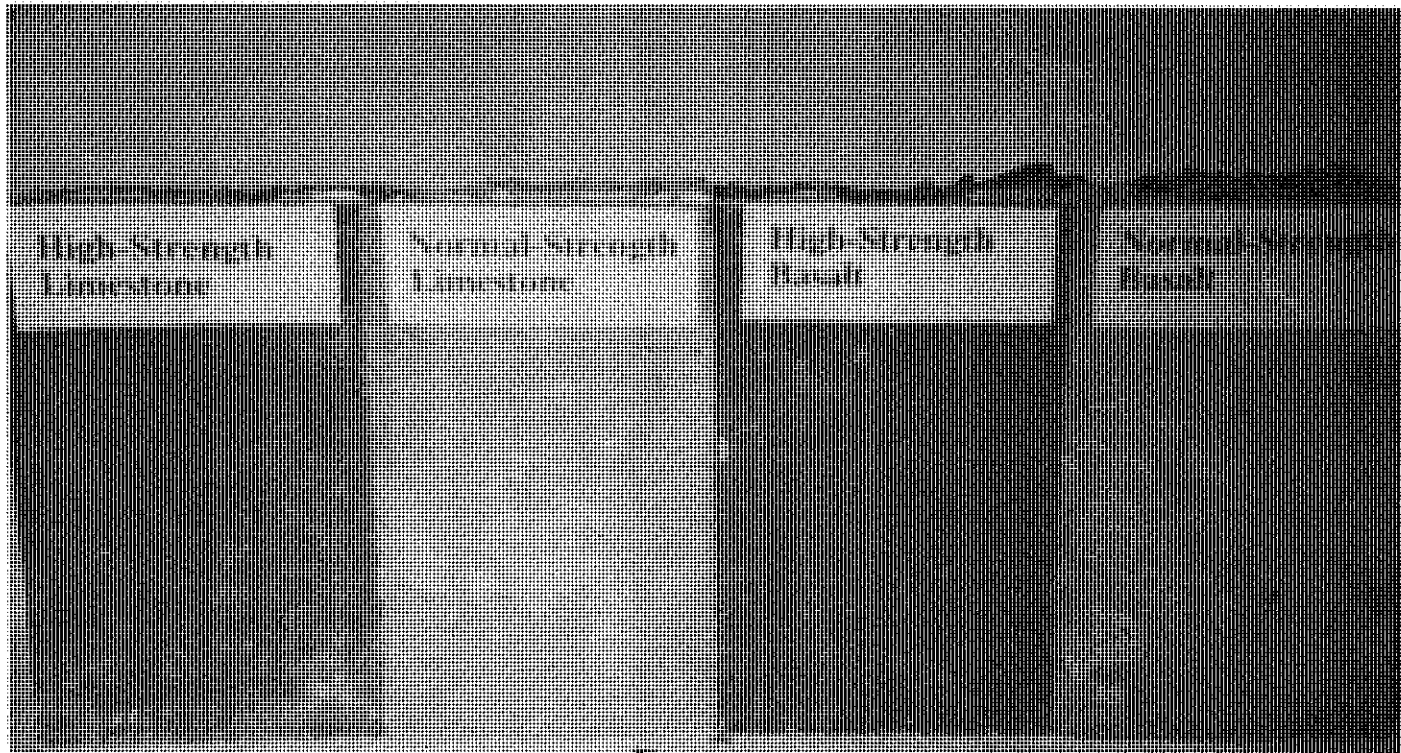


Figure 3.5 Profile of fracture surfaces for basalt and limestone normal and high-strength concretes -- 12 mm (1/2 in.) high aggregate content.

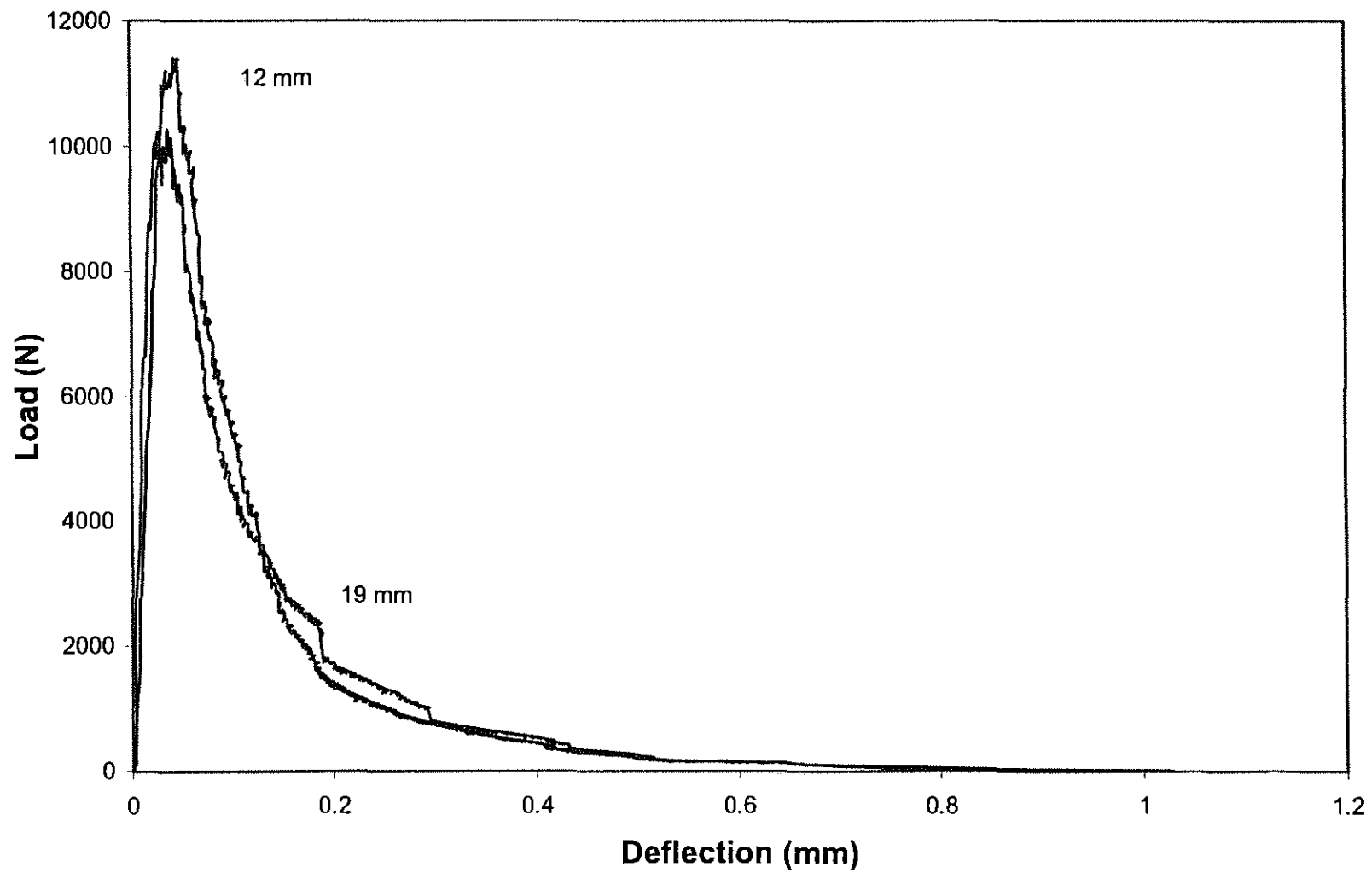


Figure 3.6 Fracture specimen load-deflection curves for 12 mm (1/2 in.) and 19 mm (3/4 in.) basalt high-strength concrete -- high aggregate content. (HB-12h.2 and HB-19h.1)

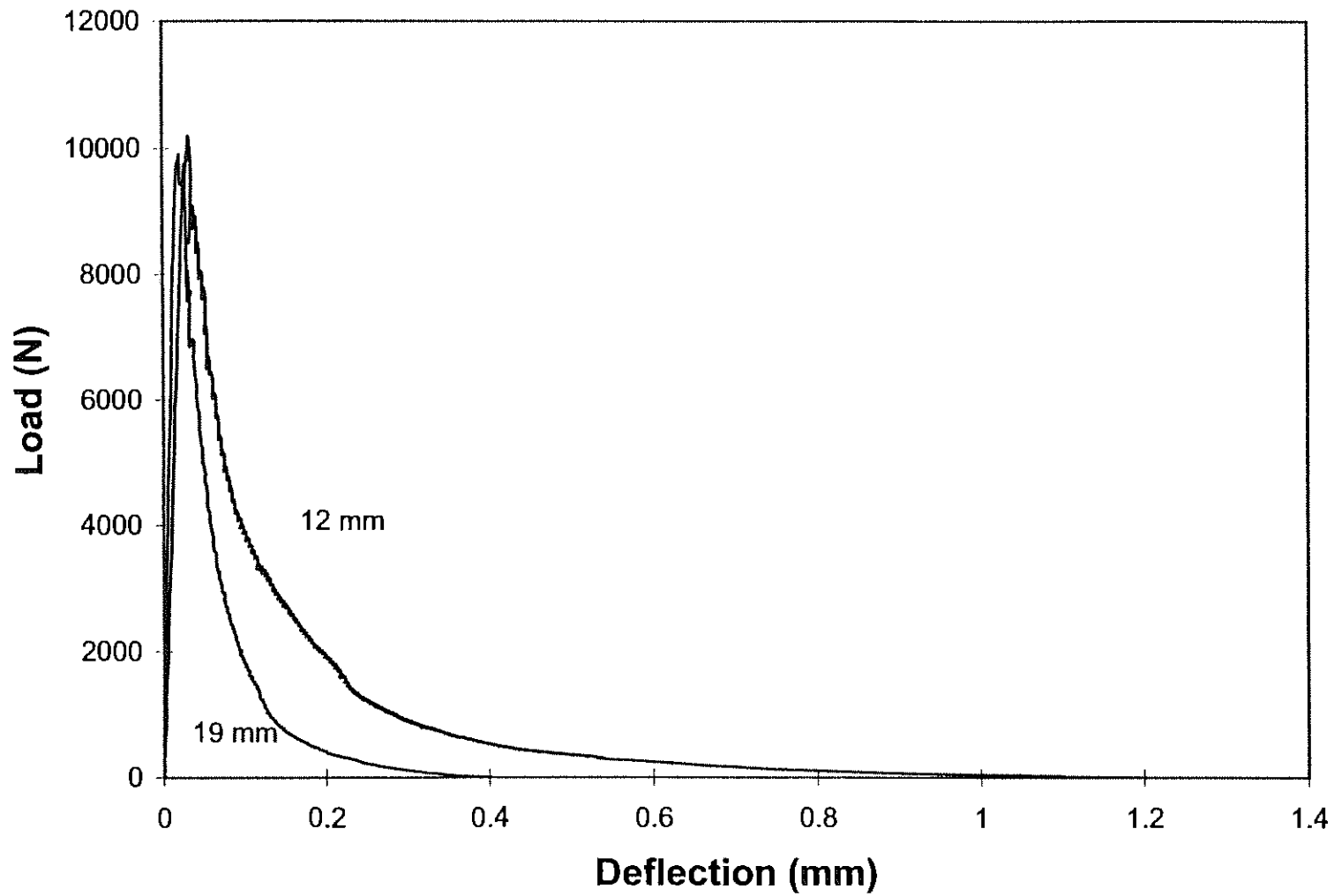


Figure 3.7 Fracture specimen load-deflection curves for 12 mm (1/2 in.) and 19 mm (3/4 in.) basalt high-strength concretes -- high aggregate content. (HB-12h.3 and HB-19h.2)

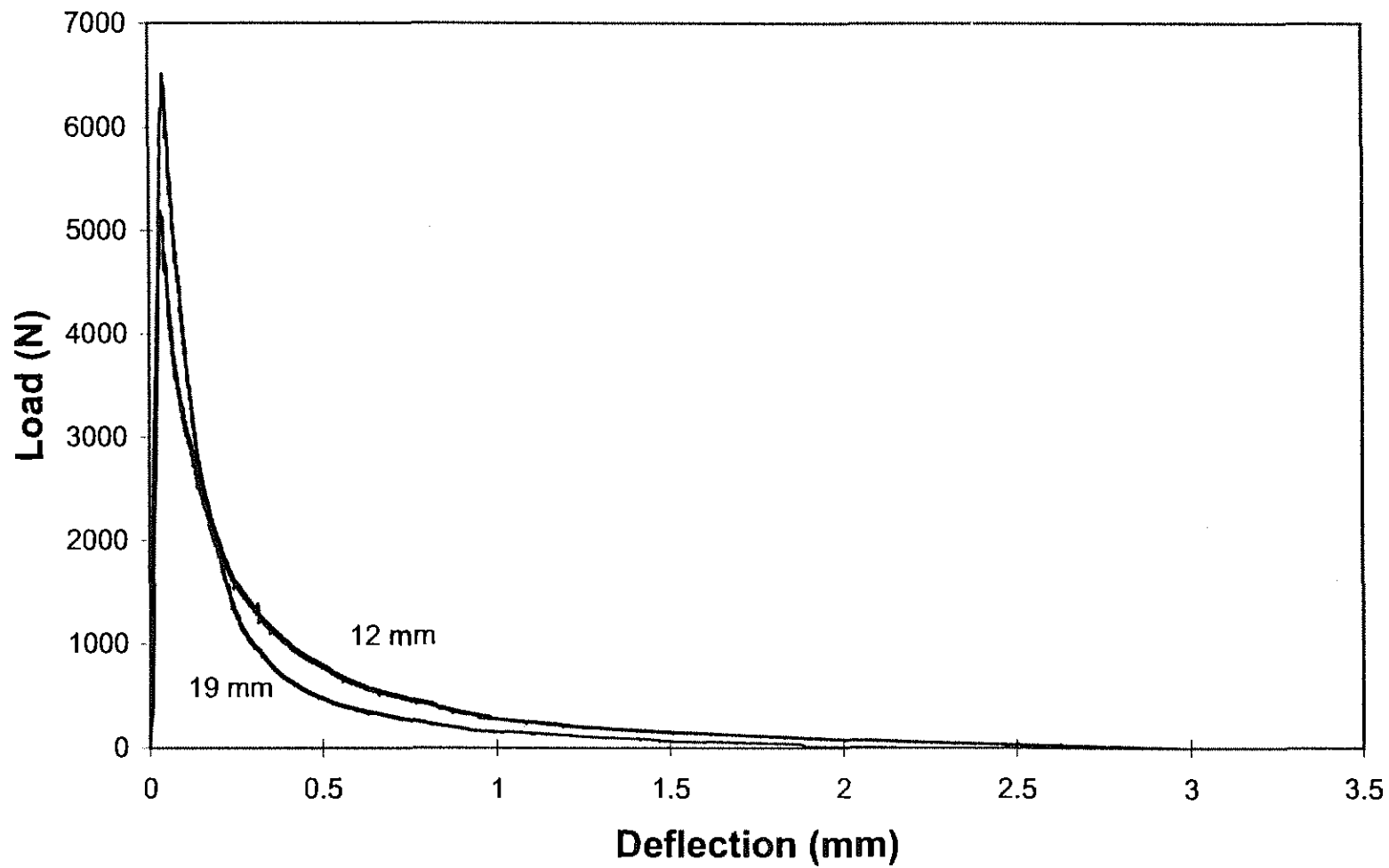


Figure 3.8 Fracture specimen load-deflection curves for 12 mm (1/2 in.) and 19 mm (3/4 in.) basalt normal-strength concretes -- high aggregate content. (NB-12h and NB-19h)

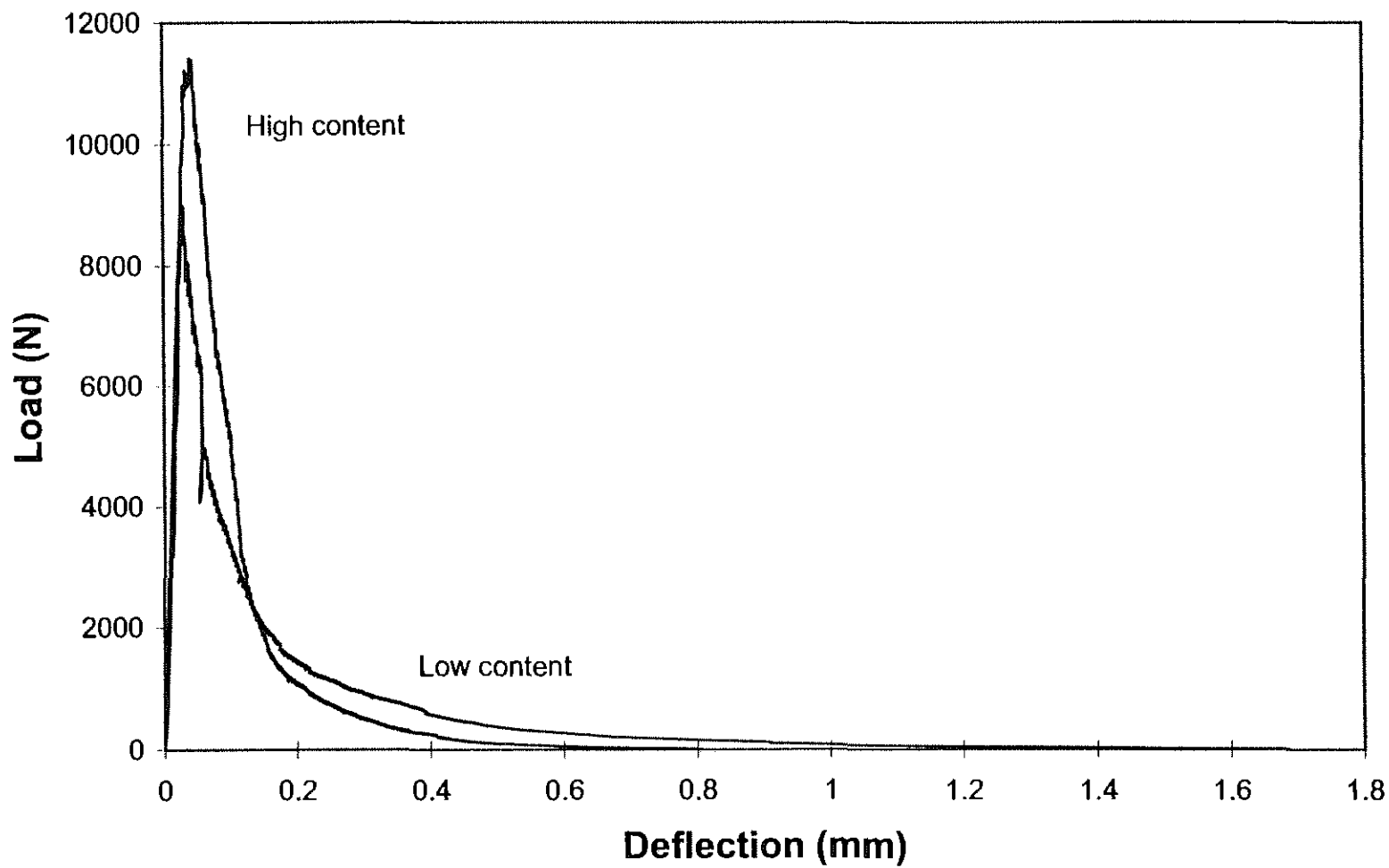


Figure 3.9 Fracture specimen load-deflection curves for high and low basalt aggregate contents -- high-strength concrete. (HB-12h.1 and HB-12l.1)



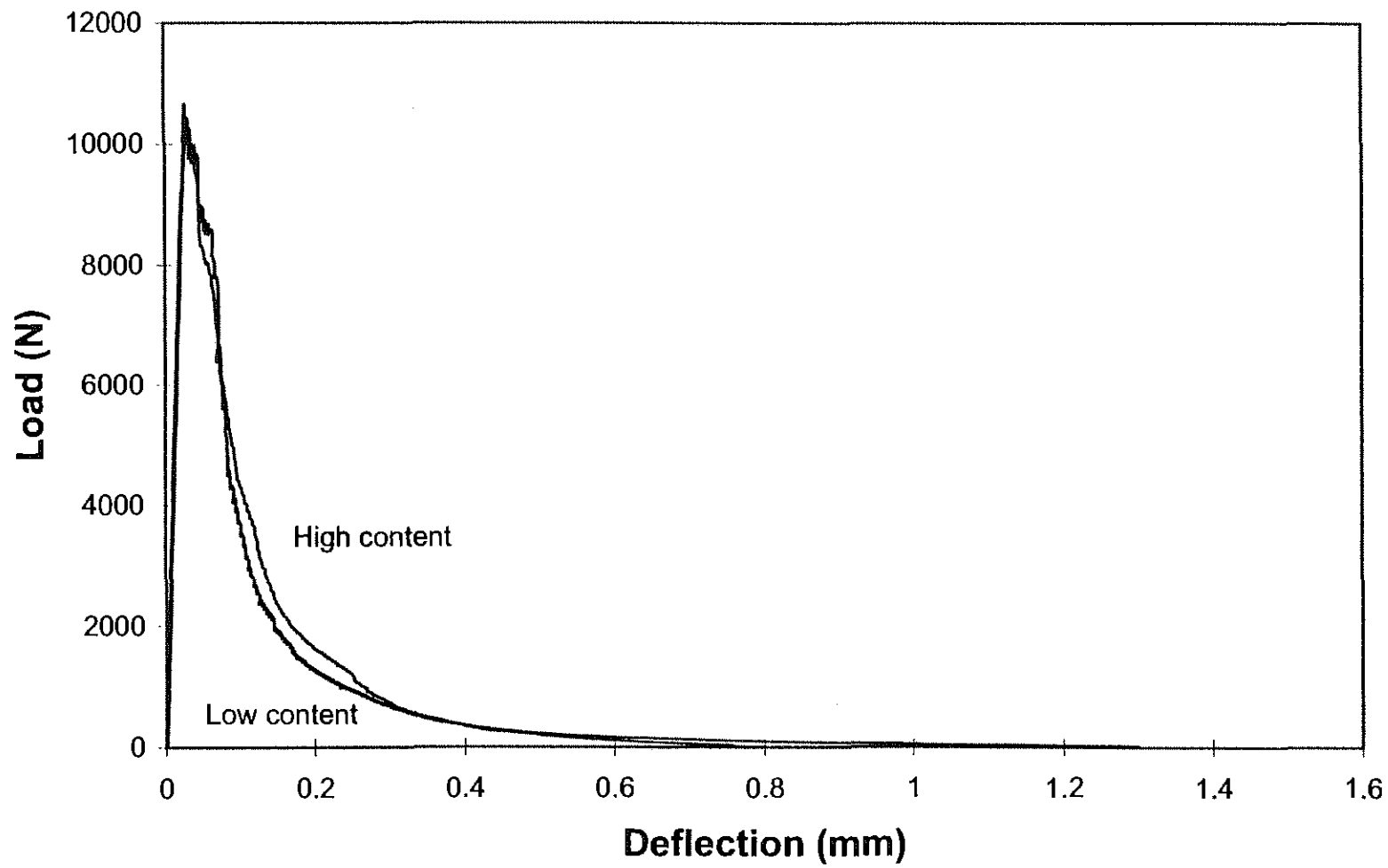


Figure 3.10 Fracture specimen load-deflection curves for high and low basalt aggregate contents -- high-strength concrete. (HB-12h.3 and HB-12l.2)

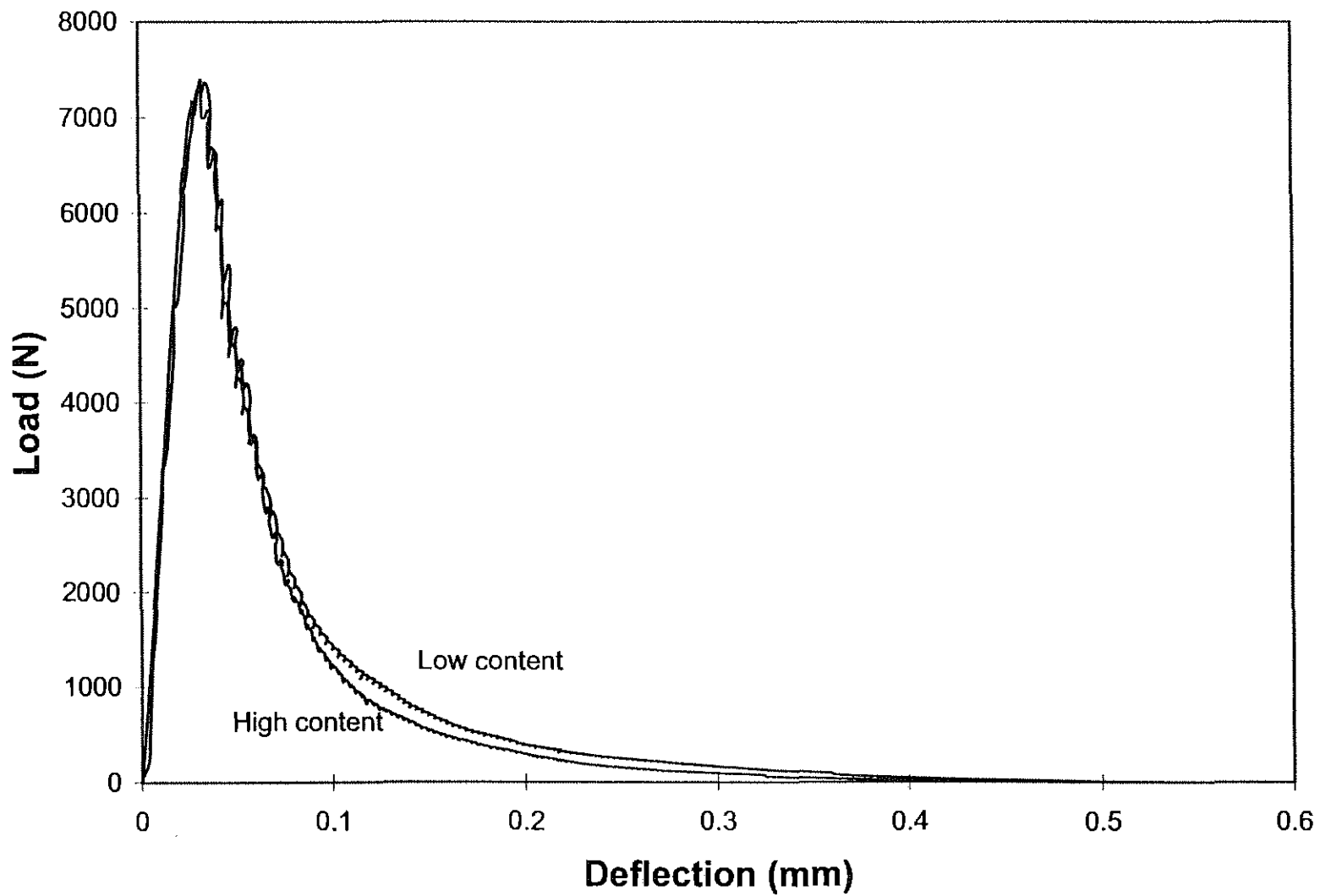


Figure 3.11 Fracture specimen load-deflection curves for high and low limestone aggregate contents -- high-strength concrete. (HL-12h.2 and HL-12l)

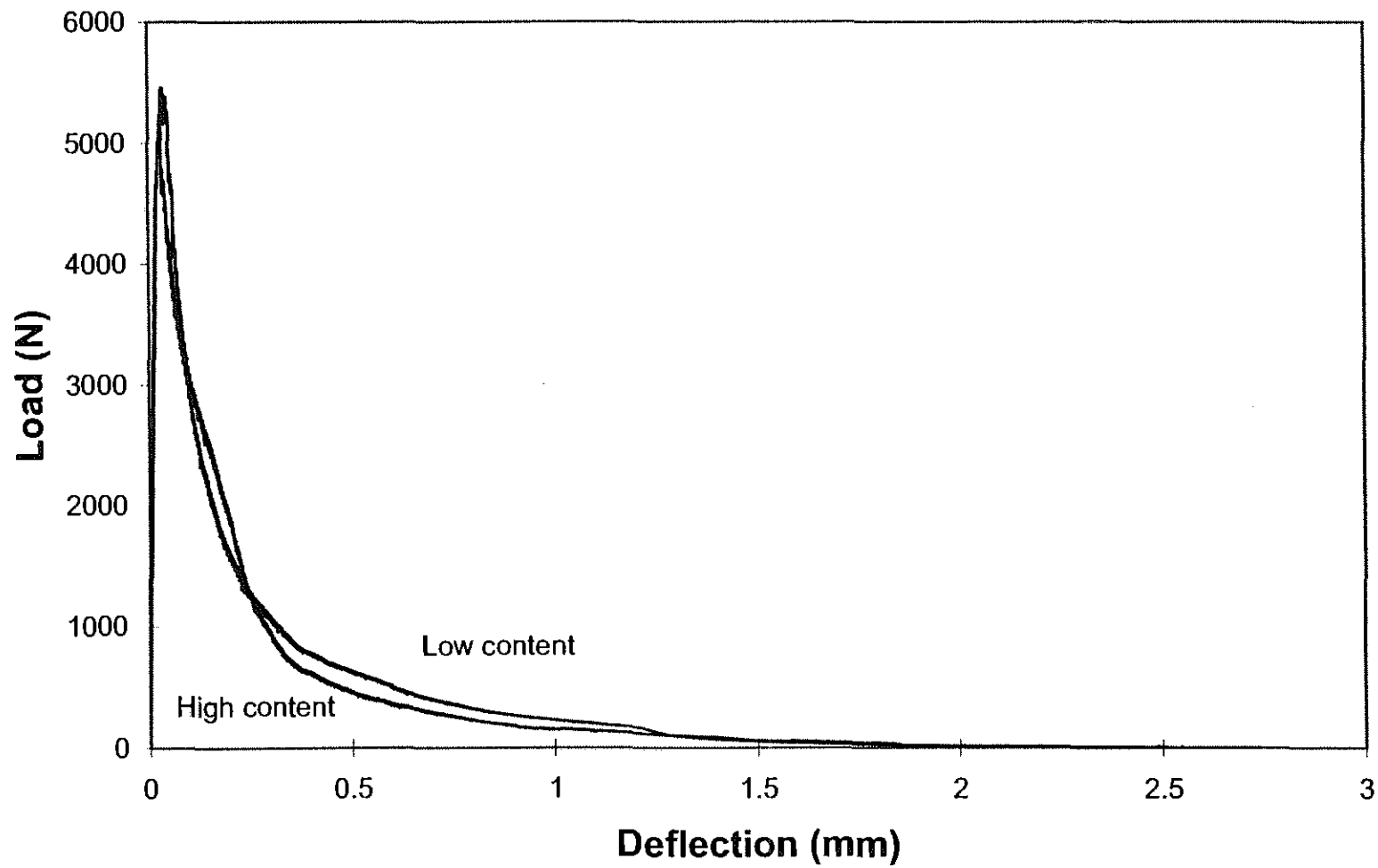


Figure 3.12 Fracture specimen load-deflection curves for high and low basalt aggregate contents -- normal-strength concrete. (NB-12h and NB-12l)

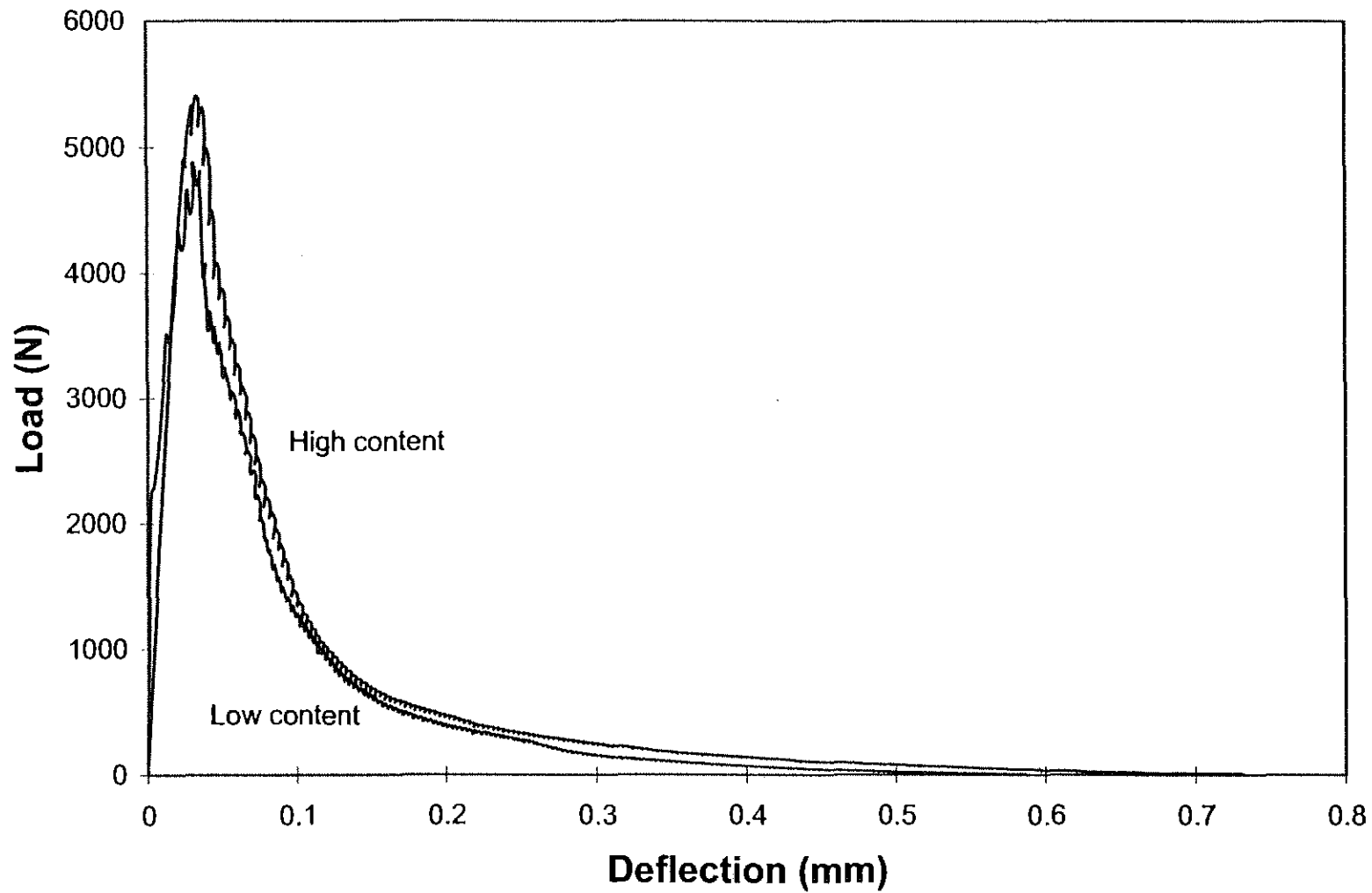


Figure 3.13 Fracture specimen load-deflection curves for high and low limestone aggregate contents -- normal-strength concrete. (NL-12h and NL-12l)

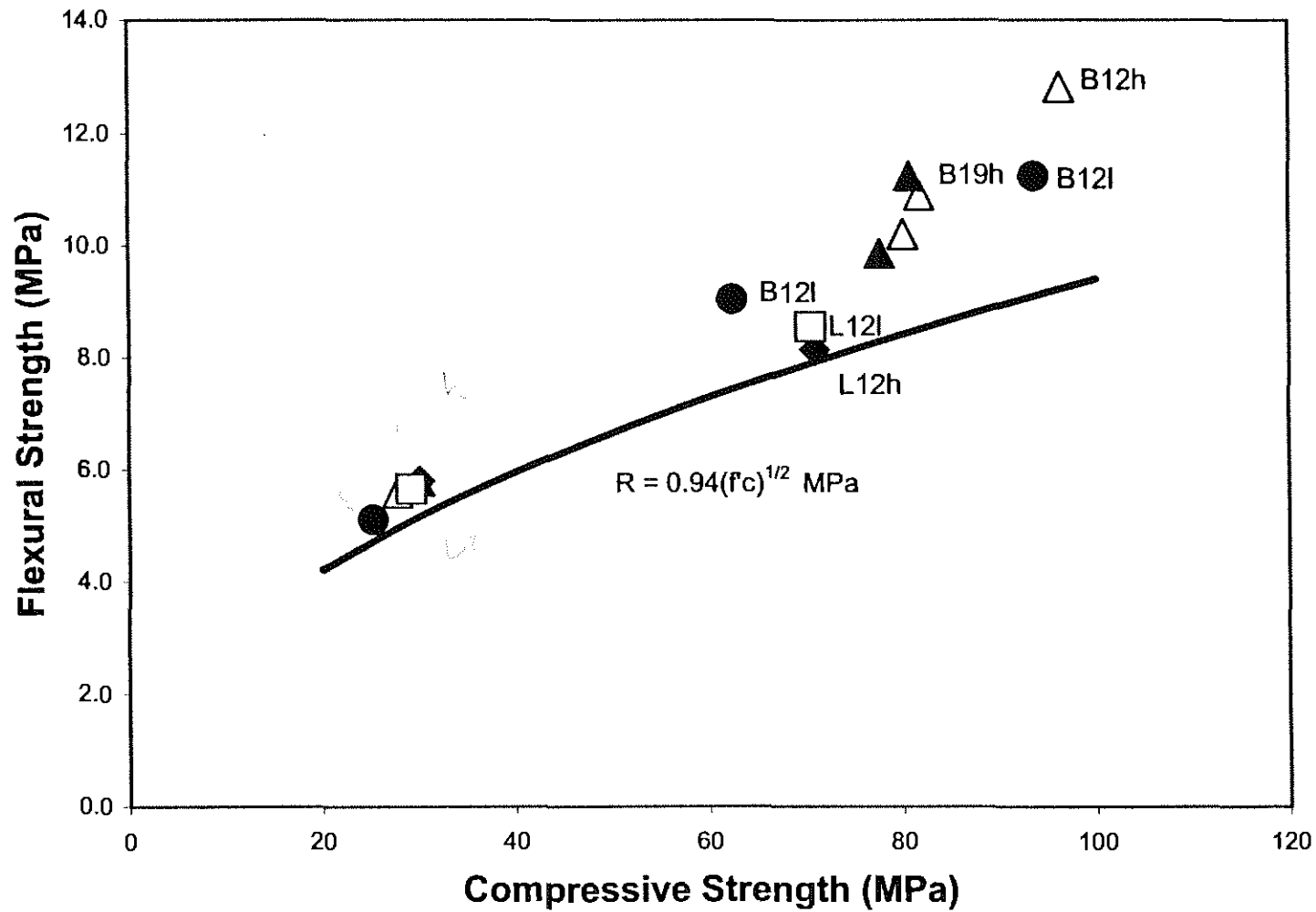


Figure 3.14 Flexural strength versus compressive strength for normal and high-strength concretes.  
 \*B=basalt; L=limestone; 12=12 mm; 19=19 mm; h=high aggregate content; l=low aggregate content.

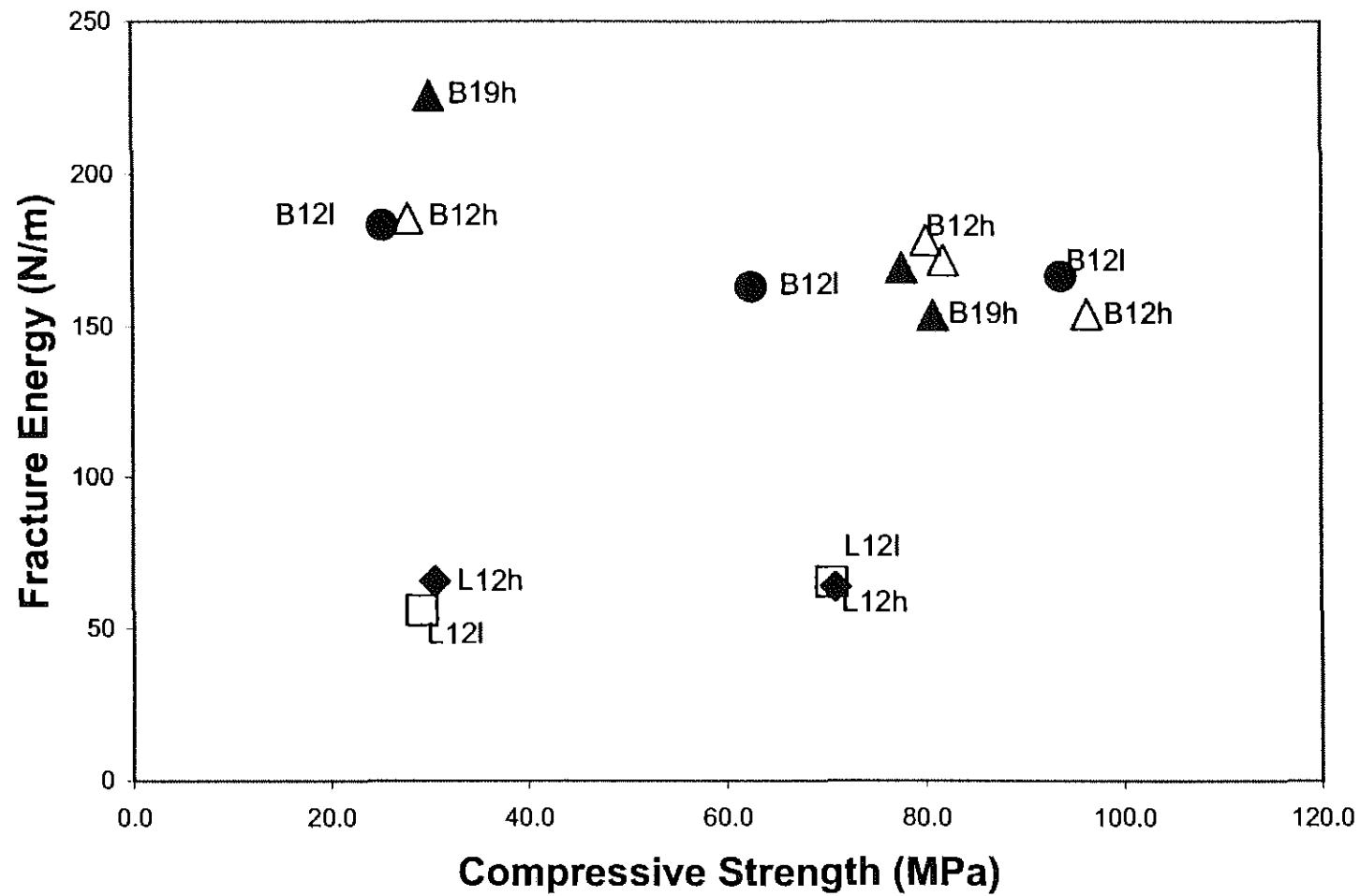


Figure 3.15 Fracture energy versus compressive strength for normal and high-strength concretes.  
 \* B=basalt; L=limestone; 12=12 mm; 19=19 mm; h=high aggregate content; I=low aggregate content.

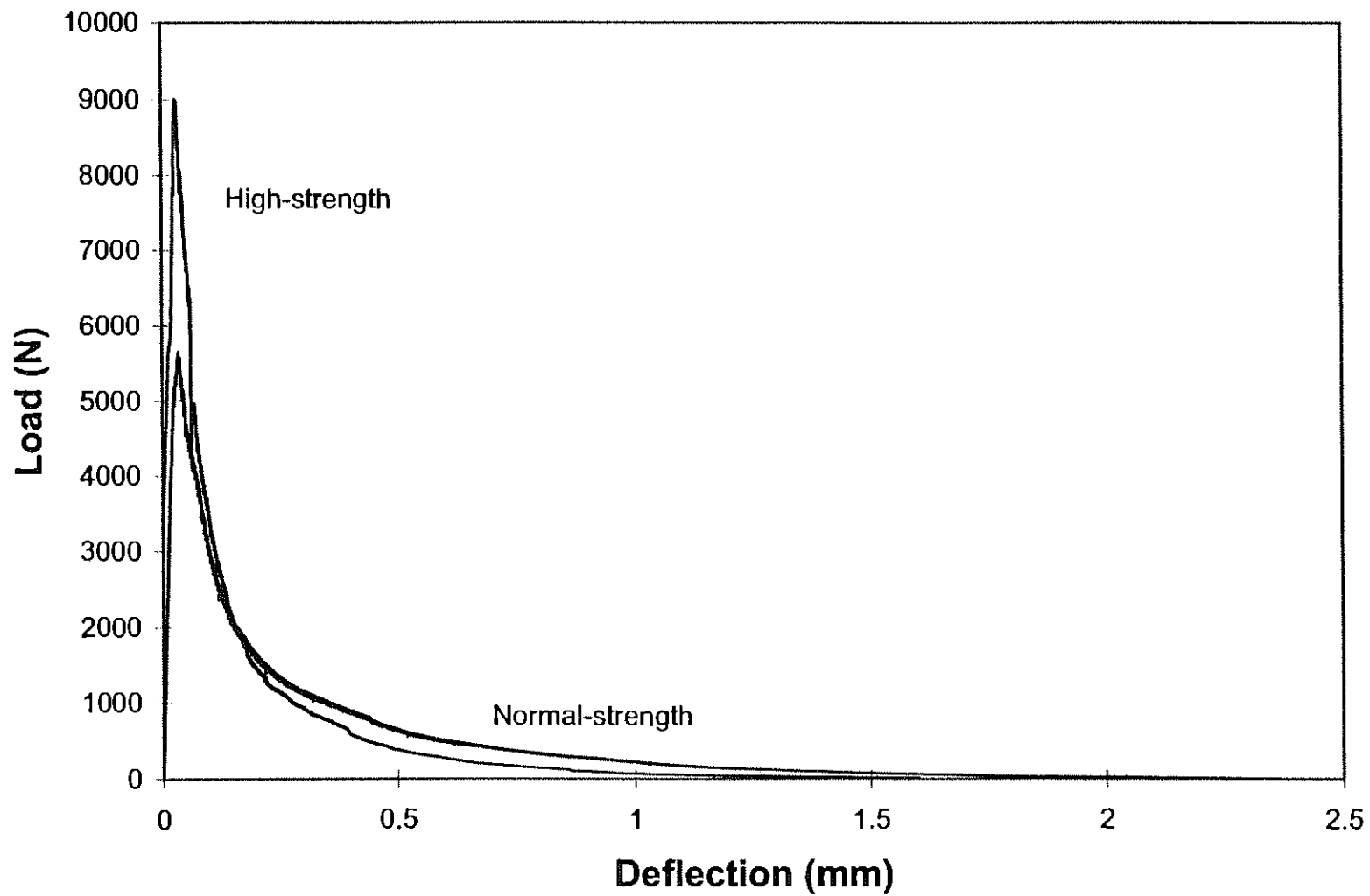


Figure 3.16 Fracture specimen load-deflection curves for normal and high-strength concretes containing 19 mm (3/4 in.) basalt --high aggregate content. (HB-19h.1 and NB-19h)

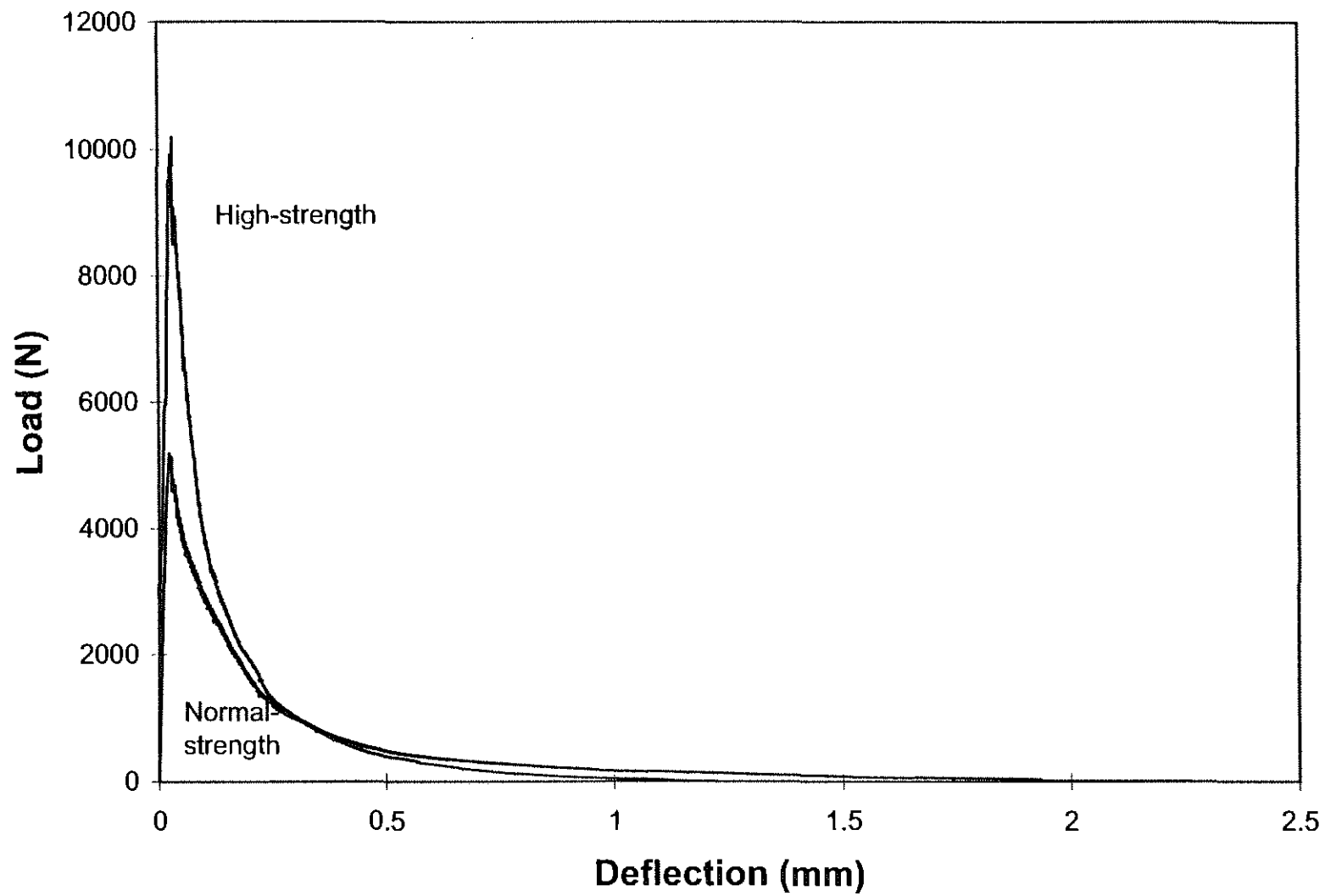


Figure 3.17 Fracture specimen load-deflection curves for normal and high-strength concretes containing 12 mm (1/2 in.) basalt -- high aggregate content. (HB-12h.3 and NB-12h)



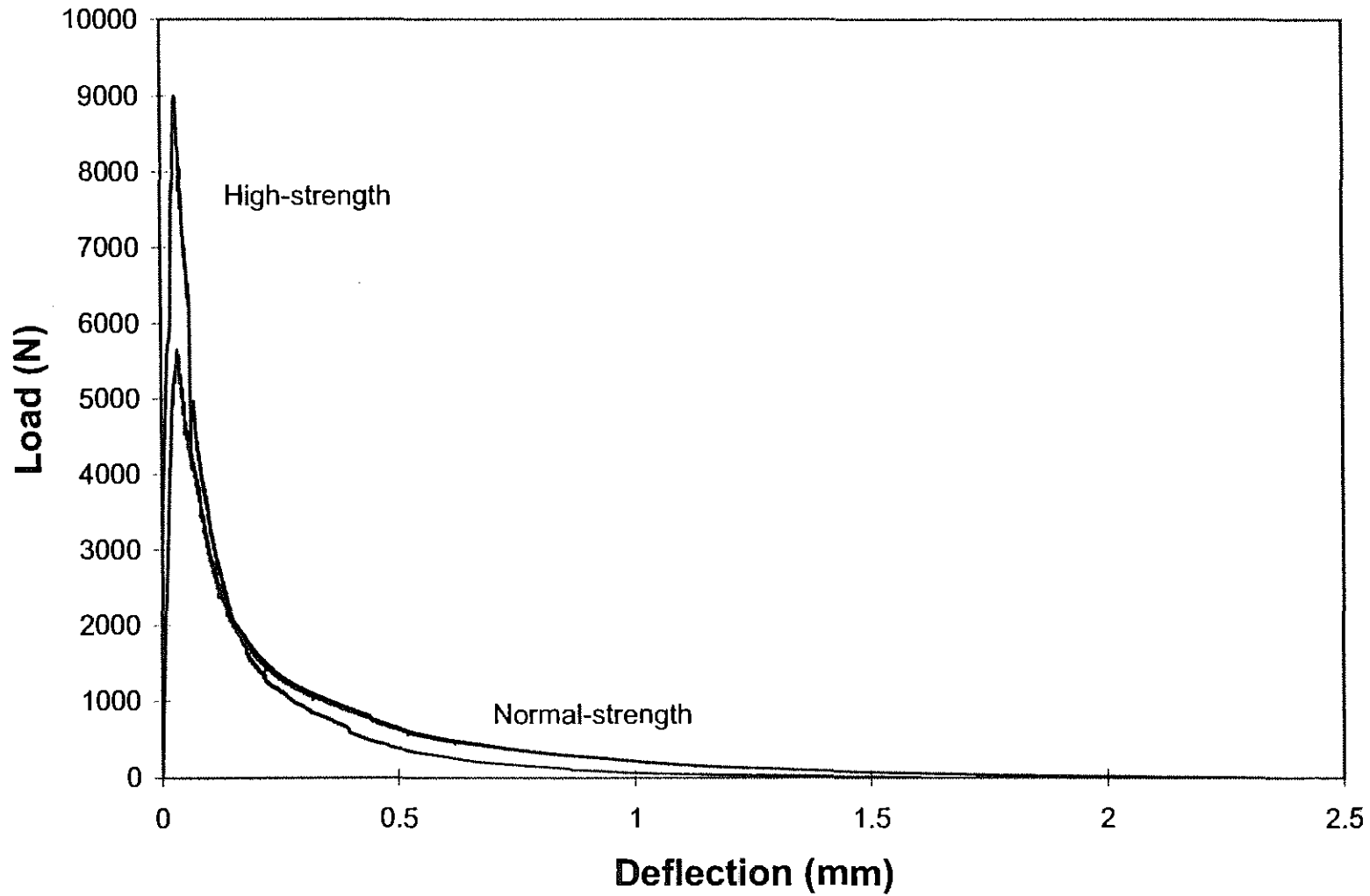


Figure 3.18 Fracture specimen load-deflection curves for normal and high-strength concretes containing 12 mm (1/2 in.) basalt -- low aggregate content. (HB-12I.2 and NB-12I)

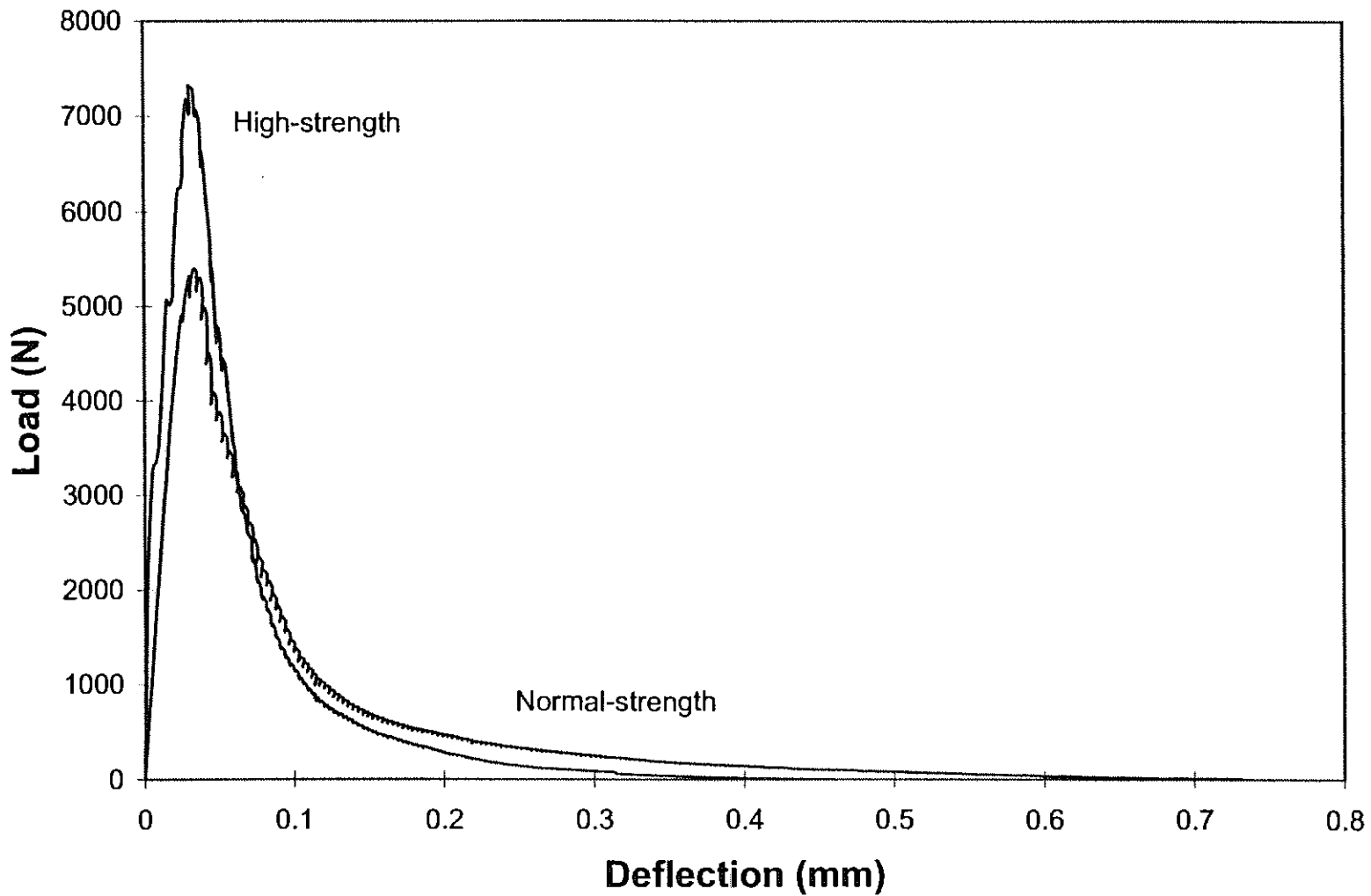


Figure 3.19 Fracture specimen load-deflection curves for normal and high-strength concretes containing 12 mm (1/2 in.) limestone -- high aggregate content. (HL-12h.2 and NL-12I)

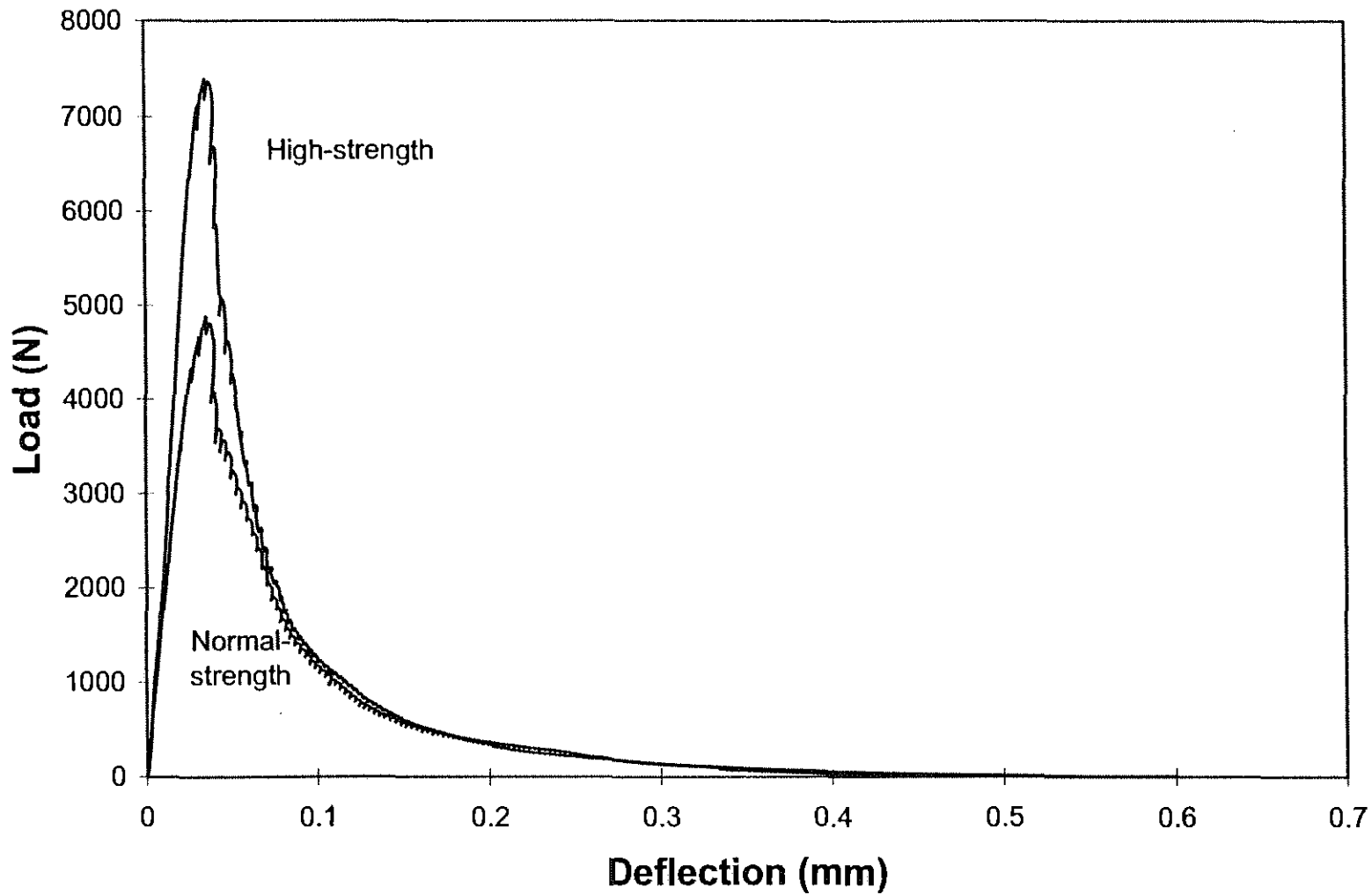


Figure 3.20 Fracture specimen load-deflection curves for normal and high-strength concretes containing 12 mm (1/2 in.) limestone --low aggregate content. (HL-12I and NL-12I)

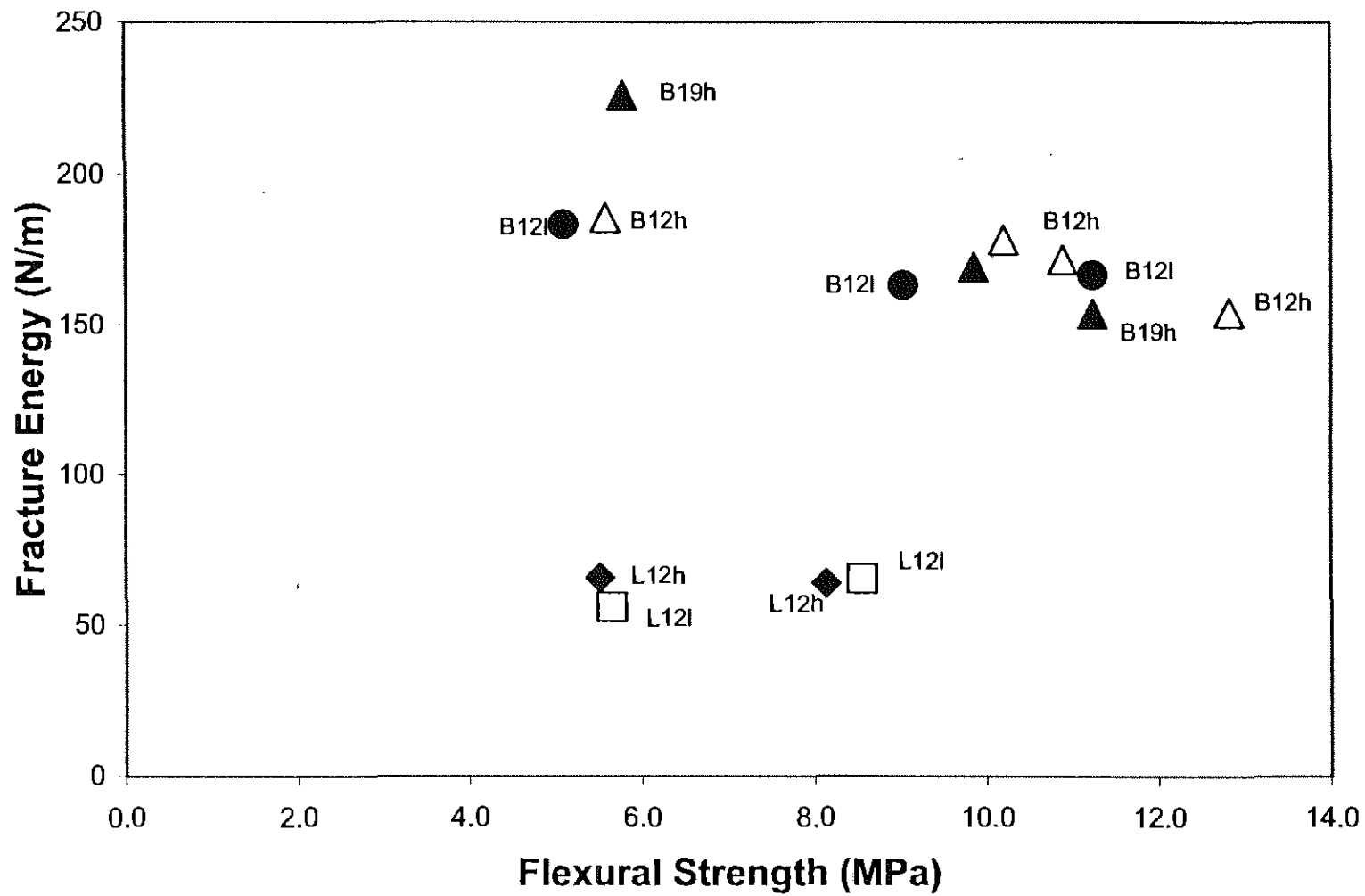


Figure 3.21 Fracture energy versus flexural strength for normal and high-strength concretes.  
 \*B=basalt; L=limestone; 12=12 mm; 19=19 mm; h=high aggregate content; l=low aggregate content.

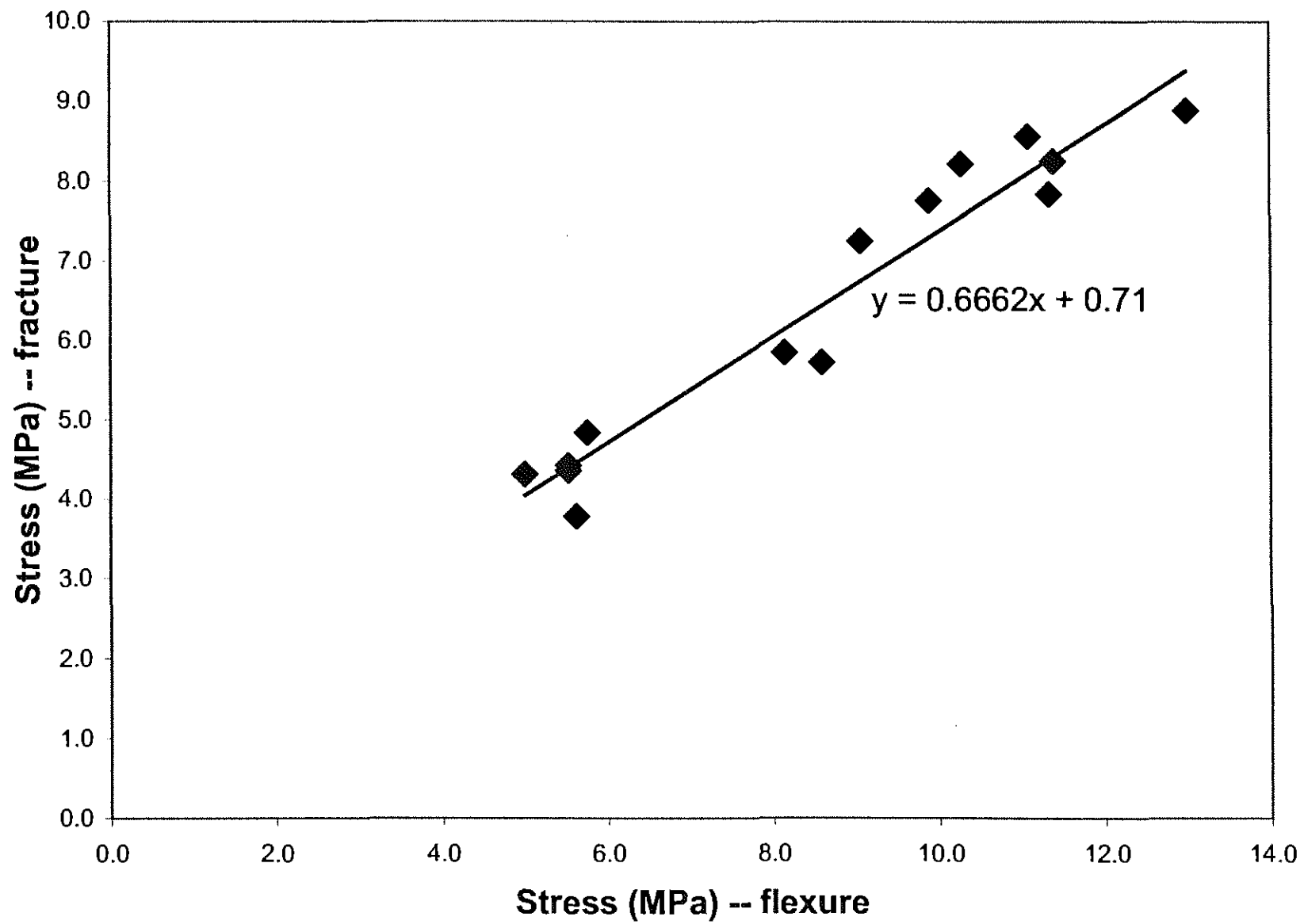


Figure 3.22 Bending stress relationship for fracture and flexural strength tests.

**Table A.1**  
**Fracture Energy Test Data**  
**(S.I. Units)**

<u>Group</u>	<u>Peak Load</u> (N)	<u>Deflection*</u> (mm)	<u>Wo</u> (m-N)	<u>Area</u> (mm <sup>2</sup> )	<u>m1</u> (kg)
HB-19h.1	9,899	0.863	1.00	7658	7.7
	10,801	0.945	0.99	7813	
	11,201	1.818	1.32	7819	
HB-19h.2	10,574	1.524	1.57	7865	7.7
	9,147	1.266	1.00	7839	
	10,263	0.701	1.12	7742	
HB-12h.1	11,588	0.796	1.09	7833	7.8
	12,081	0.876	1.18	7645	
	10,668	0.879	1.11	7839	
HB-12h.2	9,921	1.218	1.21	7742	7.7
	11,357	1.369	1.39	7710	
	11,837	1.087	1.09	7806	
HB-12h.3	11,405	1.027	1.26	7813	7.8
	11,054	1.300	1.52	7865	
	9,321	1.146	1.09	7651	
HB-12l.1	10,103	1.330	1.20	7865	7.7
	x	x	x	x	
	x	x	x	x	
HB-12l.2	8,996	1.686	1.11	7845	7.6
	10,090	2.038	1.43	7826	
	8,956	1.247	0.92	7961	
HL-12h.2	7,912	0.486	0.50	7845	7.6
	7,316	0.486	0.44	7613	
	7,374	0.415	0.43	7865	
HL-12l	7,396	0.531	0.49	7787	7.4
	7,418	0.526	0.49	7742	
	7,294	0.417	0.42	7774	

<u>Group</u>	<u>Peak Load</u> (N)	<u>Deflection*</u> (mm)	<u>Wo</u> (m-N)	<u>Area</u> (mm <sup>2</sup> )	<u>m1</u> (kg)
NB-19h	6,529	2.034	1.67	7968	7.7
	5,658	3.057	1.50	7916	
	6,516	2.963	1.54	7806	
NB-12h	6,241	3.884	1.18	7703	7.5
	5,192	2.259	1.08	7658	
	5,414	3.067	1.28	7658	
NB-12l	5,458	2.741	1.17	7573	7.4
	5,645	2.363	1.23	7677	
	5,565	2.465	1.19	7728	
NL-12h	6,276	0.730	0.49	7884	7.5
	5,396	0.731	0.46	7781	
	5,427	0.592	0.42	7800	
NL-12l	4,876	0.599	0.36	7651	7.5
	5,103	0.577	0.32	7632	
	4,640	0.697	0.44	7503	

For all tests:                    I = 0.3048 m  
    L = 0.3556 m  
    m2 = 0.227 kg

\*at failure

**Table A.2**  
**Fracture Energy Test Data**  
**(Customary Units)**

<u>Group</u>	<u>Peak Load</u> (lb)	<u>Deflection*</u> (in.)	<u>Wo</u> (in-lb)	<u>Area</u> (in <sup>2</sup> )	<u>m1</u> (lb/g)
HB-19h.1	2,227	0.034	8.83	11.9	0.53
	2,430	0.037	8.80	12.1	
	2,520	0.072	11.68	12.1	
HB-19h.2	2,379	0.060	13.90	12.2	0.53
	2,058	0.050	8.83	12.2	
	2,309	0.028	9.93	12.0	
HB-12h.1	2,607	0.031	9.66	12.1	0.53
	2,718	0.035	10.46	11.9	
	2,400	0.035	9.83	12.2	
HB-12h.2	2,232	0.048	10.72	12.0	0.53
	2,555	0.054	12.30	11.9	
	2,663	0.043	9.67	12.1	
HB-12h.3	2,566	0.040	11.20	12.1	0.53
	2,487	0.051	13.43	12.2	
	2,097	0.045	9.69	11.9	
HB-12l.1	2,273	0.052	10.67	12.2	0.53
	x	x	x	x	
	x	x	x	x	
HB-12l.2	2,024	0.066	9.82	12.2	0.52
	2,270	0.080	12.64	12.1	
	2,015	0.049	8.11	12.3	
HL-12h.2	1,780	0.019	4.43	12.2	0.52
	1,646	0.019	3.92	11.8	
	1,659	0.016	3.83	12.2	
HL-12l	1,664	0.021	4.35	12.1	0.51
	1,669	0.021	4.35	12.0	
	1,641	0.016	3.76	12.0	



<u>Group</u>	<u>Peak Load</u> (lb)	<u>Deflection*</u> (in.)	<u>Wo</u> (in-lb)	<u>Area</u> (in <sup>2</sup> )	<u>m1</u> (lb/g)
<b>NB-19h</b>	1,469	0.080	14.79	12.4	0.53
	1,273	0.120	13.24	12.3	
	1,466	0.117	13.62	12.1	
<b>NB-12h</b>	1,404	0.153	10.44	11.9	0.51
	1,168	0.089	9.59	11.9	
	1,218	0.121	11.33	11.9	
<b>NB-12I</b>	1,228	0.108	10.39	11.7	0.51
	1,270	0.093	10.86	11.9	
	1,252	0.097	10.55	12.0	
<b>NL-12h</b>	1,412	0.029	4.34	12.2	0.52
	1,214	0.029	4.09	12.1	
	1,221	0.023	3.76	12.1	
<b>NL-12I</b>	1,097	0.024	3.20	11.9	0.52
	1,148	0.023	2.84	11.8	
	1,044	0.027	3.93	11.6	

For all tests:

I = 12.0 in.

L = 14.0 in.

m2 = 0.0155 lb

\*at failure

